General Disclaimer

One or more of the Following Statements may affect this Document

- This document has been reproduced from the best copy furnished by the organizational source. It is being released in the interest of making available as much information as possible.

- This document may contain data, which exceeds the sheet parameters. It was furnished in this condition by the organizational source and is the best copy available.

- This document may contain tone-on-tone or color graphs, charts and/or pictures, which have been reproduced in black and white.

- This document is paginated as submitted by the original source.

- Portions of this document are not fully legible due to the historical nature of some of the material. However, it is the best reproduction available from the original submission.

OF **COLLEGE ENGINEERING**

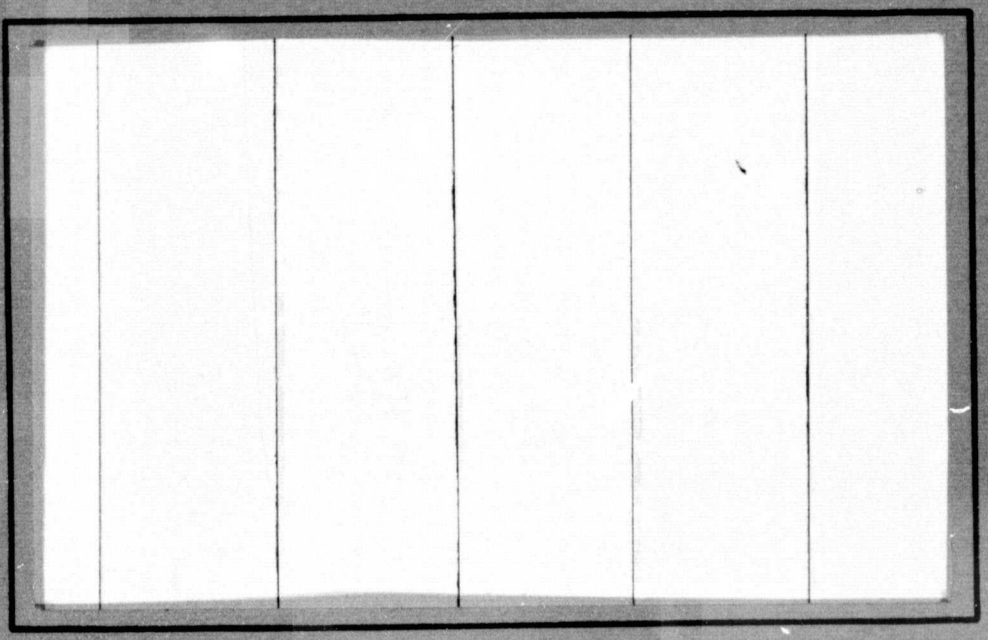

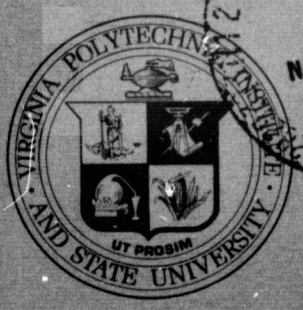

VIRGINIA POLYTECHNIC INSTITUTE AND STATE UNIVERSITY

BLACKSBURG, VIRGINIA

SEMI-ANNUAL PROGRESS REPORT

1 April 1975 through 30 September 1975

NASA - Ames Grant NSG 2016

"An Investigation of Supersonic Aeroelastic Characteristics of Oblique Winged Aircraft"

Dr. Terry A. Weisshaar, Principal Investigator
Aerospace and Ocean Engineering Department
Virginia Polytechnic Institute
and State University

Blacksburg, Virginia 24060

Introduction

This report covers progress and activity on NASA Grant NSG-2016 from 1 April 1975 through 30 September 1975. Effort during this time period had three objectives:

(a) Final development of a static aeroelastic analysis package for oblique wings in the subsonic flight regime.

(b) Improvement of the subsonic flutter analysis package with three-dimensional unsteady aerodynamics.

(c) Investigation of flutter analysis techniques suitable for the supersonic flight regimes.

Results of these efforts are discussed below.

The documentation and source deck for the static aeroelastic analysis computer program with the acronym AIRLOD was delivered to NASA Ames Research Center in May 1975. This program was forwarded to LTV - Dallas by NASA/Ames. Checkout of this program by LTV has proven satisfactory; a few minor errors were uncovered and corrected. Program extensions and improvements have been suggested, but these improvements are being held in abeyance because of more pressing problems.

Subsonic Flutter Analysis

Several improvements have been made in the subsonic flutter analysis package. Chief among these improvements is an improved, more accurate mass matrix formulation and capability to handle three rigid-body degrees of freedom. In addition, an expanded modal analysis capability was added to the program package. Checkout of the analysis package has progressed

to the point where a high confidence level in the program has been attained. A preliminary copy of this program package has been delivered to NASA/Ames for use on the Ames CDC 7600. The program was originally developed for the I.B.M. 370/158 machine.

The AIRLOD computer program and the subsonic flutter analysis computer programs have been used to generate a great deal of new numerical data. This data has formed the basis of two papers written during the summer and submitted to the AIAA Journal and AIAA Journal of Aircraft. Copies of these papers have been sent to the grant monitor and are attached to this report.

Principal Theoretical Results

Principal findings thus far have been that at least two types of flutter instability can occur in the subsonic flight regime. The first of these types of instability is associated with a low value of the ratio of wing roll moment of inertia to fuselage roll moment of inertia. This mode of instability is characterized by low reduced frequencies (k) at flutter ($k = wb/V$, where w = frequency, b = wing semi-chord and V is airspeed). This type instability involves primarily a coupling between wing elastic bending and fuselage rigid roll; this instability resembles a vehicle instability.

The second type of flutter instability involves classical bending-torsion flutter with a slight amount of rigid roll coupling. This mode of instability occurs at a relatively high reduced frequency (of the order of $k = 0.25$) and is characterized by larger values of the ratio of wing roll moment of inertia to fuselage moment of inertia. In general, if the

transition from bending-torsion flutter to bending-roll flutter can be precluded, the flutter speed of the aircraft can be kept at values far above the wing's clamped divergence speed. Research is continuing to discover the mechanism which triggers this change.

Although primary emphasis has been thus far placed on the effect of roll on the flutter of oblique wings, research has been initiated on the effect of fuselage pitch inertia on stability. The objective of this research will be to define critical parameters which may adversely couple rigid body pitch to elastic deformation.

Transient Response

It should be noted that the aerodynamic influence coefficients generated in the flutter program also may be used to solve for the transient response of the vehicle at low reduced frequency. These low reduced frequencies correspond to a slowly maneuvering vehicle. Such a study of dynamic stability and control is not currently within the scope of the present grant and is deferred to some future time. However, subsonic response of the aircraft at speeds below the critical speed is of great importance.

Supersonic Flutter Analysis

The supersonic flight regime with subsonic leading edges is, for flutter, next in importance after the high subsonic regime. Unfortunately, no one unified method seems available for the generation of supersonic aerodynamic influence coefficients. The particular difficulty which arises in the case of the subsonic leading edge is that the region between

the foremost Mach cone and the leading edges (the so-called diaphragm region) complicates the solution for velocity potential formulations.

The Mach box formulation of the supersonic flow problem presents one way of solving for the aerodynamic influence coefficients. This method has been found to have several deficiencies, the principal shortcomings being inaccuracy at low supersonic Mach numbers ($M < 1.2$) and the computational time necessary for some planform configurations. In addition, available computer codes are restricted to analyzing symmetrical planforms. A literature search has uncovered three potentially worthwhile methods for solving the supersonic problem; these methods are discussed below.

Available Solution Methods for Supersonic Flutter Analysis

A computer program is available through COSMIC which can be used to predict flutter at supersonic speeds. This program is called LAR-10199 and was developed by E. C. Yates at Langley Research Center. The analysis method used in the program is based upon so-called modified strip theory. A separate analysis of the static, rigid wing must be available to predict the spanwise distribution of lift curve slope and the chordwise position of the aerodynamic center (AC). This latter quantity is extremely important to flutter analysis. It has been noted that the failure of linearized supersonic theory to accurately predict the AC position leads to overly unconservative flutter predictions in many cases. However, Yates shows that with the proper prediction of the static AC, good results may be achieved.

A second method of supersonic flutter prediction is the use of piston theory. While piston theory is commonly used to predict flutter when $M >> 1$ or $M^2k >> 1$, a correction has been suggested to give agreement with the second-order quasi-steady supersonic theory of Van Dyke. This correction is thought to extend the validity of piston theory to lower supersonic Mach numbers and lower reduced frequency.

The Mach box method is also available for use in the flutter analysis. It appears, however, that a reprogramming of the method is necessary to account for asymmetry of the wing. This reprogramming effort does not need to be as extensive as existing Mach box programs since existing programs usually concern themselves not only with the wing pressure distribution but also with wing-tail interference effects. This latter effect is of no concern to the present analysis. An investigation of the time required for this programming effort is currently underway.

In addition to the above methods, other techniques have been suggested for calculating supersonic AIC's. Prime among these are the acceleration potential kernel function techniques. A literature survey of related papers is currently being conducted.

Planned Approach to Supersonic Flutter Analysis

Because of the disparity of analytical results often encountered in supersonic flutter analysis, the author believes it to be prudent to pursue several courses of study simultaneously. As a temporary measure, the program LAR-10199 should be obtained and made operational as quickly as possible. At the least, this method can identify, in a qualitative

manner, the flutter behavior which may be encountered in the supersonic flight of the oblique wing.

A listing of a computer program to compute piston theory AIC's with thickness effects and sweep corrections included is available at V.P.I. This program has the capability of generating aerodynamic data for a flutter program. An attempt will be made to make this program operational.

Finally, the effort necessary to generate a simple Mach box routine will be assessed, together with an investigation of newer supersonic AIC generation methods. The rationale behind the study of these methods is to generate and compare data generated by different theories and to compare differences and similarities of results.

Continuing Subsonic Flutter Work

A substantial amount of subsonic flutter investigations remain to be done. These studies include the effect of pitch inertia on flutter and the effect of shifting the wing c.g. relative to the aerodynamic center and the elastic axis. These efforts will continue; a graduate student is presently doing graduate work in this area.

Travel

During the time period covered, a trip was made to the AIAA Structures/ Structural Dynamics Meeting held in May 1975 in Denver, Colorado. In addition a visit to NASA/Ames Research Center was made on 25-26 September 1975. During this visit the latest results of subsonic oblique wing flutter studies were presented.

FLUTTER OF ASYMMETRICALLY SWEPT WINGS

by

Terrence A. Weisshaar*

and

J.B. Crittenden+

Virginia Polytechnic Institute

and State University

Blacksburg, Virginia

This research was supported by NASA Ames Research Center, Moffett Field, California under NASA Grant NSG-2016.

Index categories: Aircraft Handling, Stability and Control; Aeroelasticity; Aircraft Structural Design.

*Assistant Professor, Aerospace and Ocean Engineering Department, Member AIAA.

+Research Assistant, Aerospace and Ocean Engineering Department.

ABSTRACT

Recent interest in asymmetrically swept, or oblique, wings has raised fundamental questions about the flutter characteristics of such wings. This paper presents two formulations of the oblique wing flutter problem; one formulation allows wing bending deformations and the rigid body roll degree of freedom while the second formulation includes bending-torsional deformation and roll degrees of freedom. Flutter is found to occur in two basic modes. The first mode is associated with bending-roll coupling and occurs at low reduced frequency values. The other instability mode is primarily one of classical bending-torsion with negligible roll coupling; this mode occurs at much higher reduced frequencies. The occurrence of bending-roll coupling mode leads to lower flutter speeds while the bending-torsion mode is associated with higher flutter speeds. The ratio of the wing mass moment of inertia in roll to the fuselage moment of inertia evidently plays a major role in the determination of which of the two instabilities is critical.

Nomenclature

$[a]$ = flexibility matrix for clamped fuselage wing

c = wing chord measured perpendicular to elastic axis (Fig. 1)

$\bar{c}$ = wing chord measured parallel to the free stream direction

$c_{L\alpha}$ = 2-dimensional sectional lift-curve slope

g = structural damping parameter

i = $\sqrt{-1}$

I_o = wing roll moment of inertia at zero sweep

k = reduced frequency, $\omega c/2V_n$ or $\omega\bar{c}/2V$

R = $(I_o/I_T)\cos^2\Lambda$

V = airspeed

V_f = flutter speed

V_n = airspeed normal to swept axis, $V_n = V\cos\Lambda$

Λ = sweep angle

ρ = air density

ω = frequency of oscillation

Introduction

The recent interest in the use of an asymmetrically swept, high-aspect-ratio wing to achieve high lift-to-drag ratios has generated interest in the aeroelastic stability characteristics of such a configuration. However, the undesirable static aeroelastic behavior of symmetrically swept forward wings has prompted some caution on the part of structural engineers towards the asymmetrical wing. As a result, considerable discussion of the merits of such a design and the potential weight penalties which might be incurred has occurred. Jones and Nisbet (Ref. 1) have presented data which tends to allay some misgivings about the aeroelastic stability of asymmetrically swept or oblique wings. Prominent among their findings is the discovery that the inclusion of the rigid body aircraft roll degree of freedom has a stabilizing effect on the aeroelastic stability of the wing, when compared to the stability of a similar, but clamped, wing. Their analytical results were obtained through the use of quasi-static aerodyanmic theory to represent the perturbation lift forces generated by the harmonic motion of their idealized flexible model.

This study seeks to explore in somewhat more detail than Ref. (1) the flutter behavior of asymmetrically swept or oblique wings; to accomplish this task the results of two studies are presented. The first study examines the flutter behavior of an idealized, uniform-property wing in incompressible flow and at various asymmetrical angles to the flow. For this portion of the study, quasi-steady aerodynamic strip theory will be employed in the equations of motion; the Galerkin method will be used to solve these equations.

The second portion of the study entails the use of a more sophisticated approach to the solution of the oblique wing flutter problem. This approach uses a finite-element, unsteady aerodynamic representation together with a multi-degree-of-freedom structural model to examine more closely and more accurately the flutter behavior of variable planform wings.

From these studies, it will be shown that, at moderate sweep angles, the flutter speed of the wing may be lowered when compared with the flutter speed of the wing at zero sweep. In addition, the shape of the wing planform and the spanwise distribution of stiffness and weight will have a significant effect on the relation between flutter speed and sweep angle.

Discussion

The first part of this study is concerned with the aeroelastic analysis of a simplified oblique wing model, shown in Fig. 1. The impetus for such a study stems from the desirability of assessing the behavior of the flutter speed of the wing as it is asymmetrically swept. This model represents a wing of uniform structural and aerodyanmic properties, asymmetrically swept at an angle Λ to the flow. This high aspect ratio wing is idealized as a beam with a straight elastic axis, free to roll about an axis parallel to the flow. It is assumed that mass is distributed along this roll axis such that a mass moment of inertia, I_f, simulating the roll moment of inertia of the fuselage, appears concentrated there.

To examine the aeroelastic stability of this model, assume that it is caused to undergo small oscillations about a "wings level" static equilibrium portion. The stability of the subsequent motion can be determined by an examination of the character of this free vibration.

The structural behavior of this wing can be modelled through the use of conventional Euler-Bernoulli beam theory. It is further assumed that the wing has no torsional flexibility so that only bending flexibility is important. The limits to the validity of this latter assumption will be discussed later in this paper.

In Ref. 2 , Barmby and Cunningham discuss the flutter analysis of symmetrically swept wings through the use of aerodynamic strip theory and the Theordorsen functions. The present study neglects all the noncirculatory aerodynamic terms in Ref. 2 but retains two of the circulatory terms. In addition, the free vibratory motion is assumed to take place at a value of reduced frequency $k = \omega c/2V_n$ which is so small that the flow is quasi-steady. The circulatory aerodynamic terms retained are the term which corresponds to the familiar damping-in-roll and the term which arises from the angle of attack generated by bending deformations of a swept wing (Ref. 2).

The assumptions about the behavior of this idealized model undergoing small oscillations in the airstream lead to the following differential equation of motion for the elastic wing.

$$m\frac{\partial^2 W}{\partial t^2} + EI\frac{\partial^4 W}{\partial y^4} + (qcc_{L\alpha}\cos^2\Lambda)\frac{\partial W}{\partial y}\tan\Lambda \qquad (1)$$

$$+\left(\frac{qcc_{L\alpha}\cos^2\Lambda}{V\cos\Lambda}\right)\frac{\partial W}{\partial t} - qcc_{L\alpha}\cos^2\Lambda\left(\frac{py}{V}\right)$$

$$- m\dot{p}y\cos\Lambda = 0$$

where m = wing mass per unit length along the y-axis

EI = bending stiffness of cross-section perpendicular to y-axis

q = freestream dynamic pressure

W = wing upward deformation due to bending only

t = time

p = roll rate in radians per unit time

Nondimensionalization of Eq. (1) yields the following equation.

$$\left(\frac{mL^4}{EI}\right)\ddot{w} + \frac{\partial^4 w}{\partial \eta^4} + \lambda \frac{\partial w}{\partial \eta} - \left(\frac{\lambda}{\tan\Lambda}\right)\left(\frac{pL}{V}\right)\eta \qquad (2)$$

$$+ \left(\frac{\lambda}{\sin}\right)\left(\frac{\dot{w}L}{V}\right) - \left(\frac{mL^4}{EI}\right)(\dot{p}\cos\Lambda)\,\eta = 0$$

where $(\dot{})$ = differentiation with respect to time

$w = W/L$

$\eta = y/L$

$\lambda = qcc_{L\alpha}L^3\sin\Lambda\cos\Lambda/EI$

The requirement that the sum of all roll moments generated by wing oscillatory motion be equal to zero results in the additional equation:

$$\left(I_f + I_o\cos^2\Lambda\right)\dot{p} = \left(qcc_{L\alpha}L^2\cos^3\Lambda\right)\left(\int_{-1}^{1}\frac{\partial w}{\partial \eta}\,\eta d\eta\right)\tan\Lambda \qquad (3)$$

$$+ \left(mL^3\cos\Lambda\right)\int_{-1}^{1}\ddot{w}\eta d\eta$$

$$- \frac{2}{3}\,qcc_{L\alpha}L^2\cos^3\Lambda\left(\frac{pL}{V}\right)$$

$$+ \frac{qcc_{L\alpha}L^3\cos^2\Lambda}{V}\int_{-1}^{1}\dot{w}\eta d\eta$$

If we let $\phi = p\cos\Lambda$ then Eq. (3) may be written as

$$\ddot{\phi} + \frac{2}{3}\left(\frac{\gamma L}{V}\right)\dot{\phi} = (\gamma\sin\Lambda)\int_{-1}^{1}\frac{\partial w}{\partial \eta}\,\eta d\eta + \frac{3}{2}\left(\frac{I_W}{I_T}\right)\int_{-1}^{1}\ddot{w}\eta d\eta \qquad (4)$$

$$+ \left(\frac{\gamma L}{V}\right)\int_{-1}^{1}\dot{w}\eta d\eta$$

where $I_T = I_f + I_o\cos^2\Lambda$

$I_W = I_o\cos^2\Lambda = \frac{2}{3}mL^3\cos^2\Lambda$

$\gamma = qcc_{L\alpha}L^2\cos^3\Lambda/I_T$

To solve Eqs. (2) and (4), the time dependency is eliminated by recognition that the functions $w(\eta,t)$ and $\phi(t)$ are separable such that

$$w(\eta,t) = f(\eta)e^{rt} \tag{5a}$$

$$\phi(t) = \Phi e^{rt}$$

Next, Eq. (2) is separated into two parts, one valid in the region $-1 \leq \eta \leq 0$, the other valid in the region $0 \leq \eta \leq 1$. Finally the resulting set of equations is solved approximately through use of Galerkin's method. A simple polynomial to use for such a solution is that shape obtained for uniform loading of a cantilever beam. In this case the function $f(\eta)$ is approximated as:

$$f(\eta) = \begin{cases} \frac{a}{3}(6\eta^2 - 4\eta^3 + \eta^4) & 0 \leq \eta \leq 1 \\ \frac{b}{3}(6\eta^2 + 4\eta^3 + \eta^4) & -1 \leq \eta \leq 0 \end{cases} \tag{6}$$

where a and b are unknown constants. the Galerkin method leads to a set of three homogeneous algebraic equations, represented in matrix form as:

$$\left[d_{ij}\right]\begin{Bmatrix} a \\ b \\ \Phi \end{Bmatrix} = \begin{Bmatrix} 0 \\ 0 \\ 0 \end{Bmatrix} \tag{7}$$

The coefficients d_{ij} are given in the Appendix to this paper.

It is found that, in the absence of the roll freedom, the first natural frequency of vibration of the clamped wing, in vacuo, is predicted by the Galerkin method to be

$$\omega_o = 3.530\sqrt{\frac{EI}{mL^4}} \tag{8}$$

This compares with the exact solution (Ref. 3)

$$\omega_o = 3.518\sqrt{\frac{EI}{mL^4}} \tag{9}$$

For the clamped wing, it is found that the sweptforward wing undergoes static divergence when r is zero. This occurs at a value of λ equal to

6.40. The exact wolution gives a value of λ for static divergence of 6.33 (Ref. 4).

If all the system parameters, such as EI, Λ and V, are substituted into the expressions for d_{ij}, then the determinant of the matrix d_{ij}, written as $\Delta(d_{ij})$, can be used to find r through the relation:

$$\Delta(d_{ij}) = 0 \tag{10}$$

With reference to Eqs. (5a,b), it is seen that if r is found to be a real number, then motion is aperiodic. A positive real value of r indicates aperiodic instability or static divergence. On the other hand, if r is found to be a complex number, motion is harmonic. If $r = \alpha + i\omega$ then the motion is periodic of frequency ω. For negative values of α, the motion decays, but for positive values of α it grows with time. This latter situation corresponds to the dynamic aeroelastic instability commonly referred to as wing flutter. At the value $r = i\omega$, the system undergoes undamped oscillation and is said to be in neutral equilibrium. For a given set of system parameters, the airspeed V at which this occurs is called the flutter speed, V_F.

The way in which the problem is presently formulated allows us to pick one system parameter as the unknown in Eq. (10). The magnitude of the complex number r is of no interest, but rather the value of velocity at which neutral stability occurs. For this reason, it is found to be advantageous to let $r = i\omega$ in the expressions for d_{ij} and to express these coefficients in terms of ω_o and the parameter β, defined as

$$\beta = \lambda/\lambda_{div} \tag{11a}$$

where

$$\lambda_{div} = 32/5 = 6.40 \tag{11b}$$

The expressions for d_{ij} in terms of these parameters may be found in the Appendix.

Given the system physical parameters, the determinant in Eq. (10) may be expressed in terms of the independent variable β. Collecting terms, the determinant is found to have a real part and an imaginary part given respectively by the expressions

$$\left(\frac{\omega}{\omega_o}\right)^4\left[1-\frac{39}{40}R\right]-\left(\frac{\omega}{\omega_o}\right)^2\left[2\left(1-\frac{39}{80}R\right)+\frac{\psi D}{30}+D^2\omega_o^2\left(1-\frac{39}{40}R\right)\right] \tag{12a}$$

$$+\left[1-\beta^2+\frac{26}{25}\beta R+\frac{41}{60}\psi D\right]=0$$

and

$$\left(\frac{\omega}{\omega_o}\right)^4\left(1-\frac{77}{80}R\right)-\left(\frac{\omega}{\omega_o}\right)^2\left(1+\frac{1}{40}R+\frac{1}{120}\psi U\right) \tag{12b}$$

$$+\frac{R}{2}\left(1+\beta^2/25\right)=0$$

where

$$D^2\omega_o^2=\frac{104}{405}\left(\frac{\rho c c_{L\alpha} L}{2m}\right)\left(\frac{\beta R}{\tan\Lambda}\right) \tag{13a}$$

and

$$\psi D=\frac{104}{305}\left(\frac{\rho c c_{L\alpha} L}{2m}\right)\left(\frac{R}{\tan\Lambda}\right) \tag{13b}$$

The selection of a value of β which yields identical values of the ratio ω/ω_o in Eqs. (12a,b) completes the solution. From this value of β, the flutter velocity may be obtained.

The above solution procedure was implemented for a small model wing constructed of aluminum sheet with a constant thickness of 0.064 inches. The wing properties were taken to be:

Material density = 0.101 $lb_m/in.^3$

c = 4 in. $\quad$ L = 20 in. $\quad$ $c_{L\alpha} = 2\pi$

$I_o/I_f = 3$ $\quad$ EI = 874.0 lb_f-in.

Using a sea level air density value, Eqs. (12a),(b) were solved numerically using a Newton's method trial and error solution technique. The results of this analysis are shown in Fig. 2.

From Fig. 2, it is seen that the flutter speed decreases as the wing is swept. For small values of Λ, the value of V_F greatly exceeds that of the clamped wing static divergence speed, V_D. However, as Λ increases, the critical speeds V_F and V_D draw closer together; at $\Lambda = 90°$ they will coincide. As suggested by Jones and Nisbet in Ref. 1, the moment of inertia ratio I_W/I_T plays a significant role in the flutter analysis of this asymmetrical wing. From the expression for I_W/I_T, it is clearly seen that this ratio tends to zero as Λ approaches 90°. It has been suggested that this mass moment of inertia ratio should be as large as possible to improve flutter performance. The results in Fig. 2 support this suggestion.

Since one of the original assumptions of the present analysis was that the flutter instability occurs at relatively small values of reduced frequency k it is worthwhile to note the values of reduced frequency for which the instabilities in Fig. 2 occur. These numbers are listed in Table I. Although these reduced frequencies are reasonably small, the accuracy of these results is probably somewhat degraded by the quasi-steady flow assumption.

The model just analysed is similar to, but not identical to, a series of models used by Papadales (Ref. 5) in wind tunnel experiments at Virginia Polytechnic Institute. Those experiments had as their primary objective the study of the static aeroelastic characteristics of clamped oblique wings. However, when those tests were completed, simple flutter tests were conducted on roll-free models. Although no attempt to take accurate data was made during these flutter demonstration tests, the velocity magnitudes shown in Fig. 2 correspond to the order of magnitude of the velocities observed in these demonstrations. In addition, for

sweep angles greater than 15-20°, the primary mode of instability was observed to be a fundamental symmetrical bending mode coupled with a rigid body roll oscillation (Ref. 5).

For sweep angles less than about 20°, the tests described in Ref. 5 found a flutter mode which resembled a more conventional bending-torsion coupling with a slight degree of rigid body roll interaction. These observations, together with the desire to obtain a more accurate versatile analysis model, suggested the application of a more sophisticated analysis technique to the oblique wing flutter problem. It is to this analysis that we now turn our attention.

Conventional flutter analysis of realistic aircraft employs assumed structural deflections or mode shapes together with generalized coordinates assigned to these mode shapes. An excellent discussion of modal and non-modal matrix methods of flutter analysis is given by Rodden in Ref. 6. In addition, Ref. 6 presents a succinct discussion of how to include free-free boundary conditions into the conventional restrained or clamped model. This latter discussion follows the development given in Ref. 7, but is more general. The highlights of Ref. 6 are reviewed here.

To analyze the flutter behavior of a planform such as that shown in Fig. 4, it is necessary that the following items be taken into account: the distributed mass of the wing along the span; the variable bending and torsional stiffness along the span; and the unsteady, three-dimensional aerodynamic forces and moments associated with deformations caused by wing oscillations. With the assumption of simple harmonic motion at frequency ω, the classical matrix equation for flutter analysis, before the inclusion of assumed modes, is given by (Ref. 6):

$$\left\{h\right\} = \left(\frac{\omega^2}{1 + ig}\right)\left[a\right]\left[\left[M\right] + pb_r^2 s\left[C_h\right]\right]\left\{h\right\} \qquad (14)$$

In this equation the static flexibility matrix [a] has been divided by the factor (1 + ig) to account for the structural damping necessary to sustain simple harmonic motion. The elements of the vector {h} are actual elastic deflections and rotations at control points on the wing. The mass matrix [M] and aerodynamic influence coefficient matrix $[C_h]$ are both multiplied by the frequency squared. The coefficients of $[C_h]$ refer to the air density ρ, the reference semi-chord b_r and the wing semi-span s. The elements of $[C_h]$ are complex numbers and functions of Mach number and the local control point reduced frequency, $k = \omega b/V$, where b is the local semi-chord. With the formulation in Eq. 14, the unsteady aerodynamic forces enter into the problem, mathematically, as complex masses.

The idealization of the wing structure as an assemblage of beams, each with a straight elastic axis, permits the use of conventional finite element structural analysis methods to describe the wing stiffness and flexibility. The reader is referred to Refs. 8 and 9 for discussions of this method. Similarly, the mass matrix may be formulated from finite element methods. The mass matrix must account for the fact that the wing shear centers may be offset from the wing chordwise location of the centers of mass. Finally, to model the three-dimensional aerodynamic forces and moments, the doublet-lattice method (Ref. 10) was used. To employ this method, an existing computer program (Ref. 11) was employed to generate aerodynamic influence coefficients.

A computer program was written to calculate the matrices in Eq. 14 using these methods. The free vibration modes for the clamped system are then used to reduce the size of the matrix equations. The free-free boundary conditions are then introduced to "free" the clamped system described in Eq. 14; this allows rigid body roll freedom. Once these matrices have been formed, the eigenvalues and eigenvectors may be

found. Since the aerodynamic influence coefficients are functions of reduced frequency k and Mach number (in these studies, Mach number is zero), a set of eigenvalues and eigenvectors corresponding to each value of k is generated. The familiar V-g method (Ref. 3, pp. 565-568) is then used to find the value of velocity at which neutral stability occurs.

To assess the effect of torsion and unsteady aerodynamics on the flutter analysis of the oblique wing, the uniform property aluminum wing was reanalyzed. The wing is considered to have the same structural properties as before, but, in the present example, GJ is taken to be equal to 1346 lb-in. It should be noted that the flat, sheet-aluminum wing has a ratio of first bending to first torsion which is slightly higher than that common to conventional aircraft.

The analysis of the constant property wing, including roll freedom and torsional flexibility and employing the doublet-lattice method was conducted with a sixty degree-of-freedom model. These sixty degrees of freedom were obtained by considering ten control points on each wing; each control point has pitch, plunge and bending rotation elastic degrees of freedom. This model was subsequently reduced to a twenty degree-of-freedom model by using the first twenty natural modes of the system.

The results of this flutter analysis are displayed in Fig. 3 as ratios of the instability velocity (either flutter or divergence) to the velocity at which wing torsional divergence occurs at zero sweep; this latter velocity is denoted as V_{DO}.

In Fig. 3 the behavior of the wing when the fuselage is clamped is shown as the curve labelled V_D/V_{DO}. With the fuselage clamped, instability is found to occur at a reduced frequency k = 0; this is divergence. When roll freedom is allowed, and when $I_o/I_f = 3$, a dynamic instability appears; this is flutter and is shown as the curve V_F/V_{DO}. Unlike the

strip theory results, the flutter speed does not tend to infinity as Λ tends to zero. In fact, the flutter speed reaches a maximum near 15° of sweep and then declines, approaching the clamped divergence speed at a sweep angle of 60°. From an examination of the mode of instability in the analysis and from test observation, it is found that, from $\Lambda = 0°$ until near $\Lambda = 30°$, the instability resembles bending-torsion flutter such as might be observed on symmetrically swept back wings; an increasing amount of rigid body roll appears as Λ increases.

As a further illustration of the flutter behavior of oblique wings, a non-uniform wing planform, constructed in the same manner as the uniform property wing, was analyzed. This wing (Fig. 4) has a modified elliptical planform and is constructed to give, theoretically, the minimum induced drag for a given lift, given span and given root bending moment (Ref. 12). In this case, the wing-fuselage combination has a roll moment of inertia ratio $I_o/I_f = 11.69$. Fig. 5 shows the stability behavior of the clamped and roll-free wings. While the decrease in divergence speed with increasing Λ for the clamped wing shown in Fig. 4 resembles that of the uniform property wing, the behavior of the flutter speed for the nonuniform wing is much different. Once again, for large sweep angles, the decrease of flutter speed with sweep angle is seen in Fig. 5; however, the roll-free flutter speeds and clamped divergence speeds are more widely separated in Fig. 5 than in Fig. 3.

To assess the importance of the roll moment of inertia, the aeroelastic stability of the nonuniform property wing shown in Fig. 4 is again studied. However, the roll moment of inertia of the fuselage is now increased by a factor of two. The results of this study are presented in Fig. 6 and are compared to those previously obtained using the

smaller fuselage roll moment of inertia. Once again, the results are displayed as ratios of flutter speed to clamped divergence speed at zero sweep angle.

The effect of increasing the fuselage roll moment of inertia is clearly seen in Fig. 6. The flutter speeds for both moment of inertia ratios are seen to be identical until about a 15 degree sweep angle. Near this point the flutter mode for the $I_o/I_f = 5.85$ wing becomes predominantly one of fundamental bending with rigid body roll coupling. This is seen to depress the flutter speed as Λ increases.

As a final example, consider the uniform property aluminum wing. This wing has been previously analyzed using quasi-steady strip theory aerodynamics and elastic bending degrees of freedom with roll coupling. It has also been analyzed with a bending-torsion model which used the doublet-lattice aerodynamic loads. For the present example, the value of the torsional stiffness GJ is chosen to be 10 times that of the example whose results were presented in Fig. 3. The results of the present study are shown in Fig. 7, where they are compared with those presented in Fig. 3. In Fig. 7, the designation "Wing 2" refers to a uniform property wing with properties identical to those of "Wing 1" except that wing sectional torsional stiffness of Wing 2 is ten times that of Wing 1.

In Fig. 7, the relation between flutter speed and Λ for Wing 2 is seen to have a discontinuity near $\Lambda = 15°$. Increasing the value of GJ is found to have a pronounced effect on flutter speed at moderate sweep angles, but has little effect on flutter at high sweep angles. The discontinuity is believed to be caused by a sudden change in the flutter mode near 15 degrees sweep. For sweep angles beyond 15°, the results

obtained for this wing with high torsional stiffness resemble those obtained with the bending model and strip theory airloads. The reduced frequencies at the onset of flutter of Wing 2 are displayed in Table II for several sweep angles. From this table, it is seen that the flutter, which occurs primarily as a roll-bending or flapping instability, occurs at relatively low reduced frequencies when compared with the reduced frequencies which arise at the onset of bending-torsion flutter. Also, a comparison of the reduced frequencies in Tables I and II shows that the reduced frequencies at flutter in the two studies are comparable in magnitude.

Conclusions

Before summarizing the results of this paper and listing conclusions, certain features of the idealized models studied should be reviewed. These models were chosen for analysis because of past experience with wind tunnel tests. A constant thickness, sheet metal wing has a bending stiffness which is proportional to the wing chord measured perpendicular to the wing elastic axis; the torsional stiffness varies in a similar manner. This proportionality of the stiffness to the wing chord leads to bending and torsional stiffness distributions which are concave downward when plotted versus the spanwise coordinate. In actuality, the bending stiffness distribution which results from considerations of wing strength usually appears to have a concave upward distribution (cf. Ref. 3, p. 45).

The wings considered in this study had wing sectional centers of mass coincident with the shear centers; thus, there was no elastic axis-c.g. offset. Dynamic coupling was either nonexistent, as in the case of the uniform property wing, or minimal, as in the case of the variable property wing. This latter wing has a line of shear centers which is curved slightly forward when the wing is in its unswept position.

The combinations and permutations of the various parameters which affect the aeroelastic stability of an aircraft are seemingly endless. However, several conclusions may be drawn from the present studies at zero Mach number. Prominent among these conclusions is that the inclusion of the rigid body roll degree of freedom into the flutter model causes the mode of instability to change from an aperiodic instability (divergence) to an oscillatory instability (flutter). The degree to which the stability boundary is modified depends upon the sweep angle Λ and the ratio of the moments of inertia in roll of the aircraft fuselage and the wing in its unswept position.

If the wing instability appears as a coupling between the wing's fundamental bending mode and rigid body roll (the "flapping" mode), flutter speed is reduced as Λ increases. However, if the system parameters are such that flutter appears primarily as a bending-torsion coupling, the flutter speed may actually increase as the wing is swept. If the wing can be either elastically or dynamically tailored, it may be possible to avoid the flapping mode type of instability altogether.

Topics warranting further investigation include: the effect of Mach number on oblique wing flutter; the significance of elastic axis - c.g. offset; and the effect of elastic tailoring of the wing. It is anticipated that these and other studies will provide further insight into this unique aerodynamic design.

REFERENCES

1. Jones, R.T. and Nisbet, J.W., "Transonic Transport Wings — Oblique or Swept?," Astronautics and Aeronautics, Vol. 12, No. 1, January 1974, pp. 40-47.
2. Barmby, J.G., Cunningham, H.J. and Garrick, I.E., "Study of Effects of Sweep on the Flutter of Cantilever Wings," NACA Report 1014, 1951.
3. Bisplinghoff, R.L., Ashley, H. and Halfman, R.L., Aeroelasticity, Addison-Wesley, Reading, Mass., 1955, p. 77.
4. Bisplinghoff, R.L. and Ashley, H., Principles of Aeroelasticity, John Wiley and Sons, New York, 1962, p. 313.
5. Papadales, B.S., An Experimental Investigation of Oblique Wing Static Aeroelastic Phenomena, Master of Science Thesis, Virginia Polytechnic Institute and State University, Blacksburg, Virginia, 1975.
6. Rodden, W.P., "A Matrix Approach to Flutter Analysis," Sherman Fairchild Fund Paper No. FF-23, Institute of the Aeronautical Sciences, 1959.
7. Scanlan, R.H. and Rosenbaum, R., Aircraft Vibration and Flutter, Dover Publications, New York, 1968.
8. Przemieniecki, J.S., Theory of Matrix Structural Analysis, McGraw-Hill, New York, 1968.
9. Gallagher, R.H., Finite Element Analysis Fundamentals, Prentice-Hall, Englewood Cliffs, New Jersey, 1975.
10. Albano, E. and Rodden, W.P., "A Doublet-Lattice Method for Calculating Lift Distributions on Oscillating Surfaces in Subsonic Flows," AIAA Journal, Vol. 7, No. 2, February 1969, pp. 279-285.

11. Giesing, J.P., Kalman, T.P., Rodden, W.P., "Subsonic Unsteady Aerodynamics for General Configurations, Part I, Vol. I, Direct Application of the Nonplanar Doublet-Lattice Method," AFFDL-TR-71-5, November 1971. Wright-Patterson AFB, Ohio.

12. Jones, R.T., "The Spanwise Distribution of Lift for Minimum Induced Drag of Wings Having a Given Lift and a Given Bending Moment," NACA TN 2249, Washington, D.C., December 1950.

Table I - Reduced Frequency k at Flutter (Fig. 2)

$k = \omega c/2V_n$	Λ (Degrees)
0.0225	15
0.0330	30
0.0494	45
0.0587	60

Table II - Reduced Frequency k at Flutter

(Wing 2, Fig. 7)

$k = \omega \bar{c}/2V$	Λ (Degrees)
0.29	0.
0.29	7.5
0.29	15
0.022	20
0.025	25
0.028	30
0.038	45
0.045	60

Appendix

The application of Galerkin's method to Eqs. (2,3) results in the determinant in Eq. 10. The elements of the matrix $\left[d_{ij}\right]$ are given below.

$$d_{11} = -\left(\frac{\omega}{\omega_o}\right)^2 + i\omega D + 1 + \beta \tag{A1}$$

$$d_{12} = 0 \tag{A2}$$

$$d_{13} = \frac{9}{8}\left[\left(\frac{\omega}{\omega_o}\right)^2 - i\omega D\right] \tag{A3}$$

$$d_{21} = 0 \tag{A4}$$

$$d_{22} = -\left(\frac{\omega}{\omega_o}\right)^2 + i\omega D + 1 - \beta \tag{A5}$$

$$d_{23} = -\frac{9}{8}\left[\left(\frac{\omega}{\omega_o}\right)^2 - i\omega D\right] \tag{A6}$$

$$d_{31} = \omega^2(13R/30) - i\omega\psi(13/45) - (\gamma \sin\Lambda)(3/5) \tag{A7}$$

$$d_{32} = -\omega^2(13R/30) + i\omega\psi(13/45) - (\gamma \sin\Lambda)(3/5) \tag{A8}$$

$$d_{33} = -\omega^2 + i\omega\psi(2/3) \tag{A9}$$

The following definitions of terms are used in the above equations.

$D = (13/162)(\lambda L/V \sin\Lambda)$ $\qquad$ $\psi = \gamma L/V$

$R = (I_o/I_T)\cos^2\Lambda$ $\qquad$ $\lambda = qcc_{L\alpha}L^3 \sin\Lambda\cos\Lambda/EI$

$\beta = \lambda/\lambda_{cr} = 5\lambda/16$ $\qquad$ $\gamma = qcc_{L\alpha}L^2\cos^3\Lambda/I_T$

LIST OF FIGURES

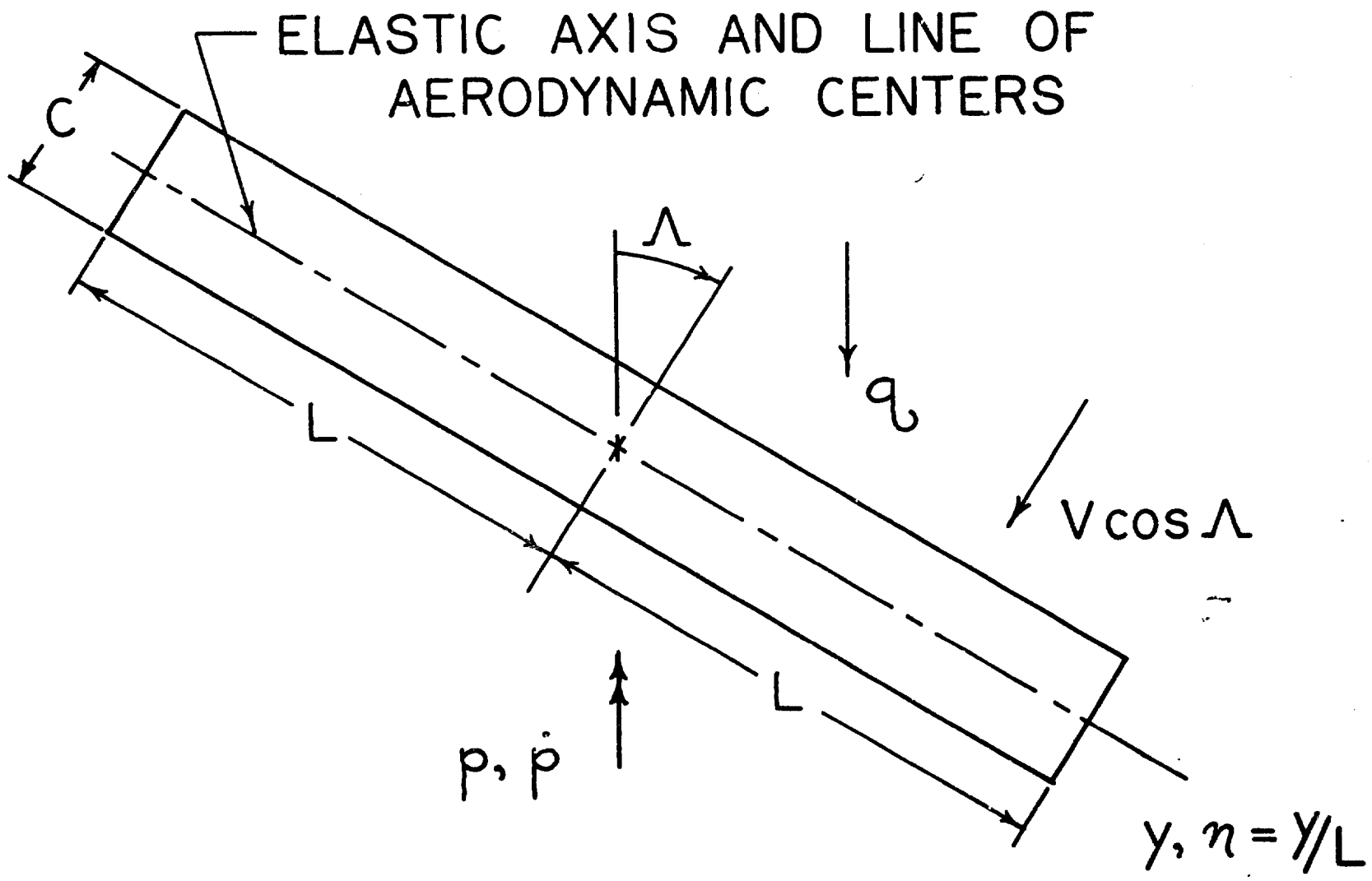

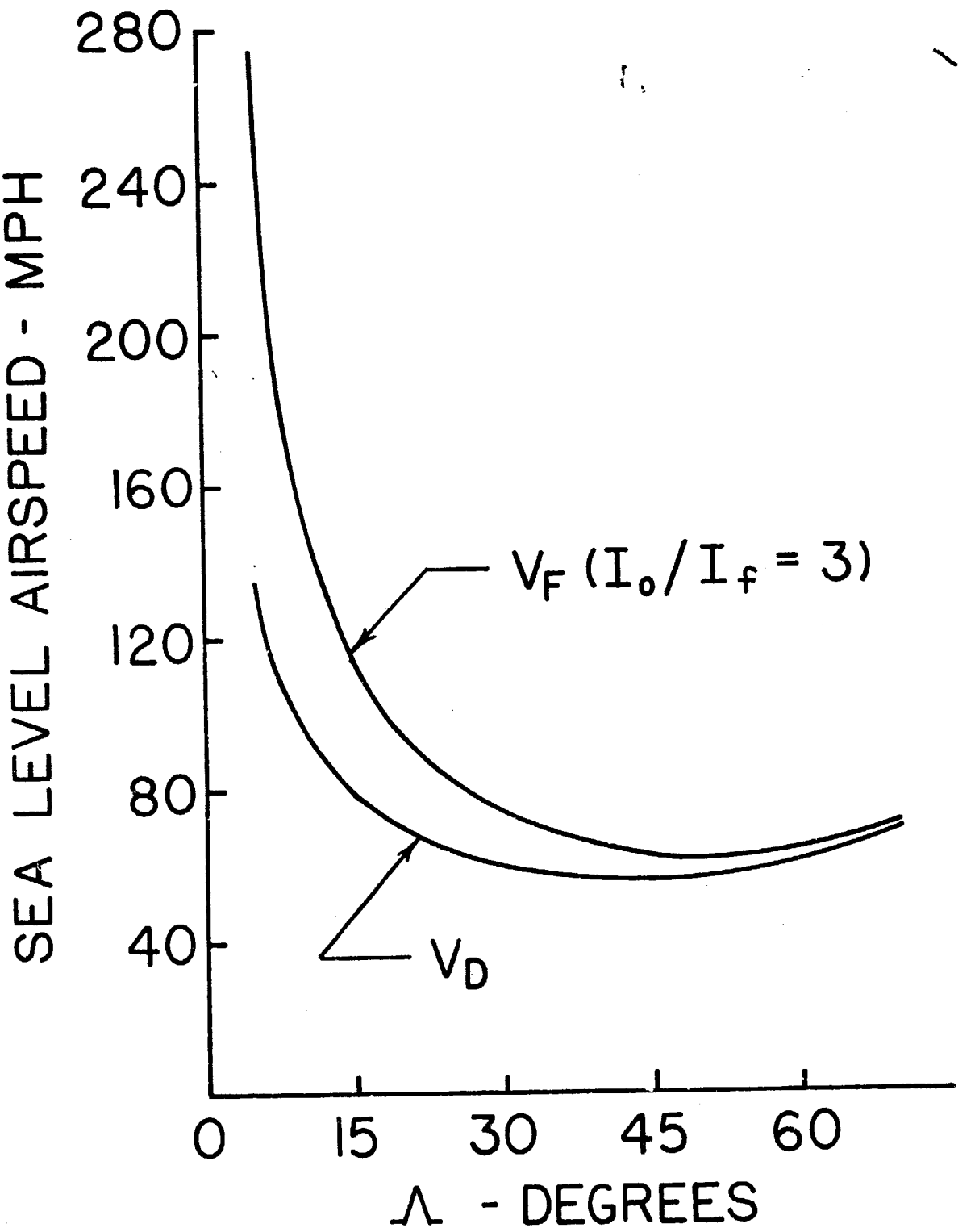
280
240
200
160
120
80
40
SEA LEVEL AIRSPEED - MPH
V_F ($I_o/I_f = 3$)
V_D
0
15
30
45
60
Λ - DEGREES

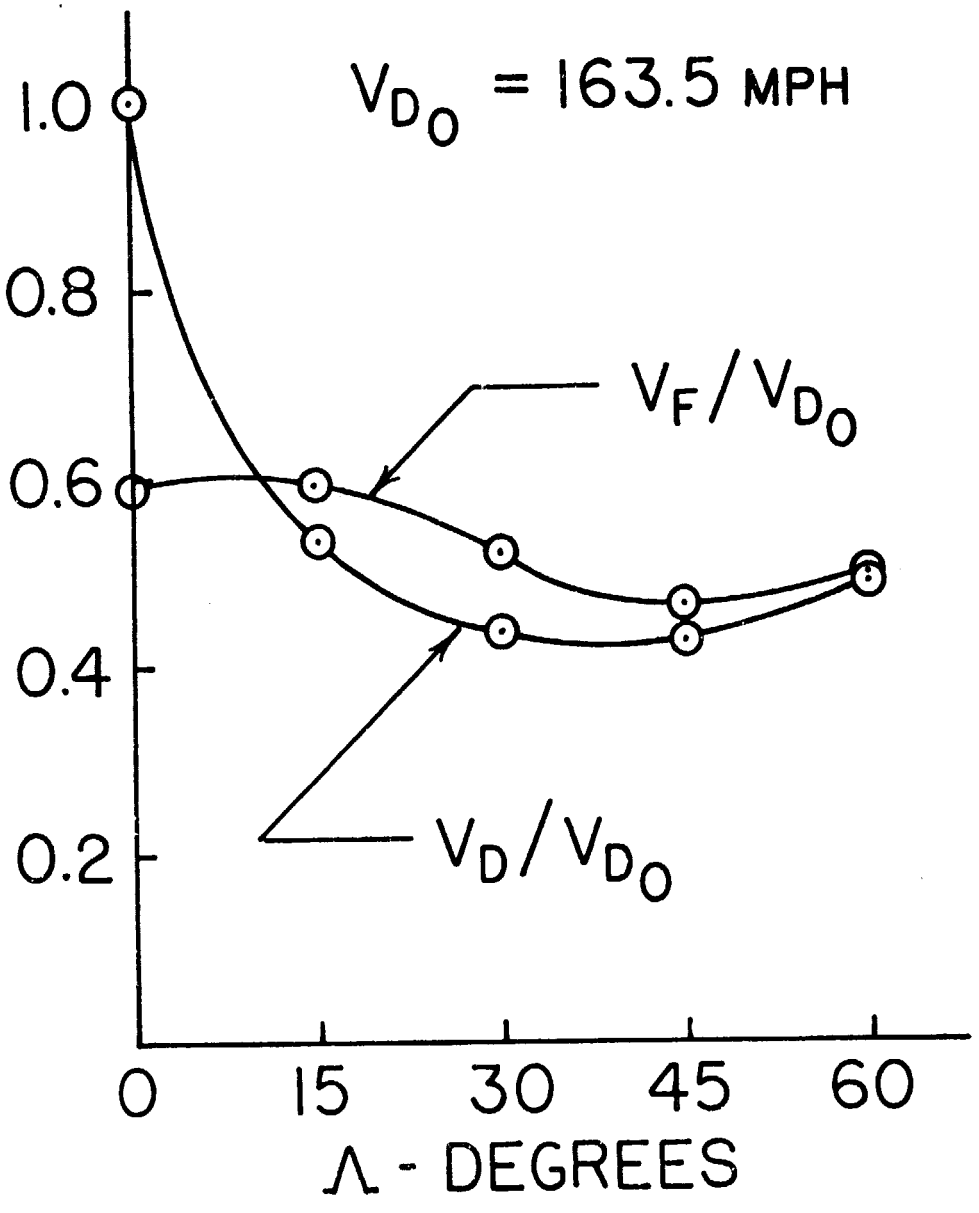
V_{D_0} = 163.5 MPH
1.0
0.8
0.6
0.4
0.2
V_F / V_{D_0}
V_D / V_{D_0}
0
15
30
45
60
Λ - DEGREES

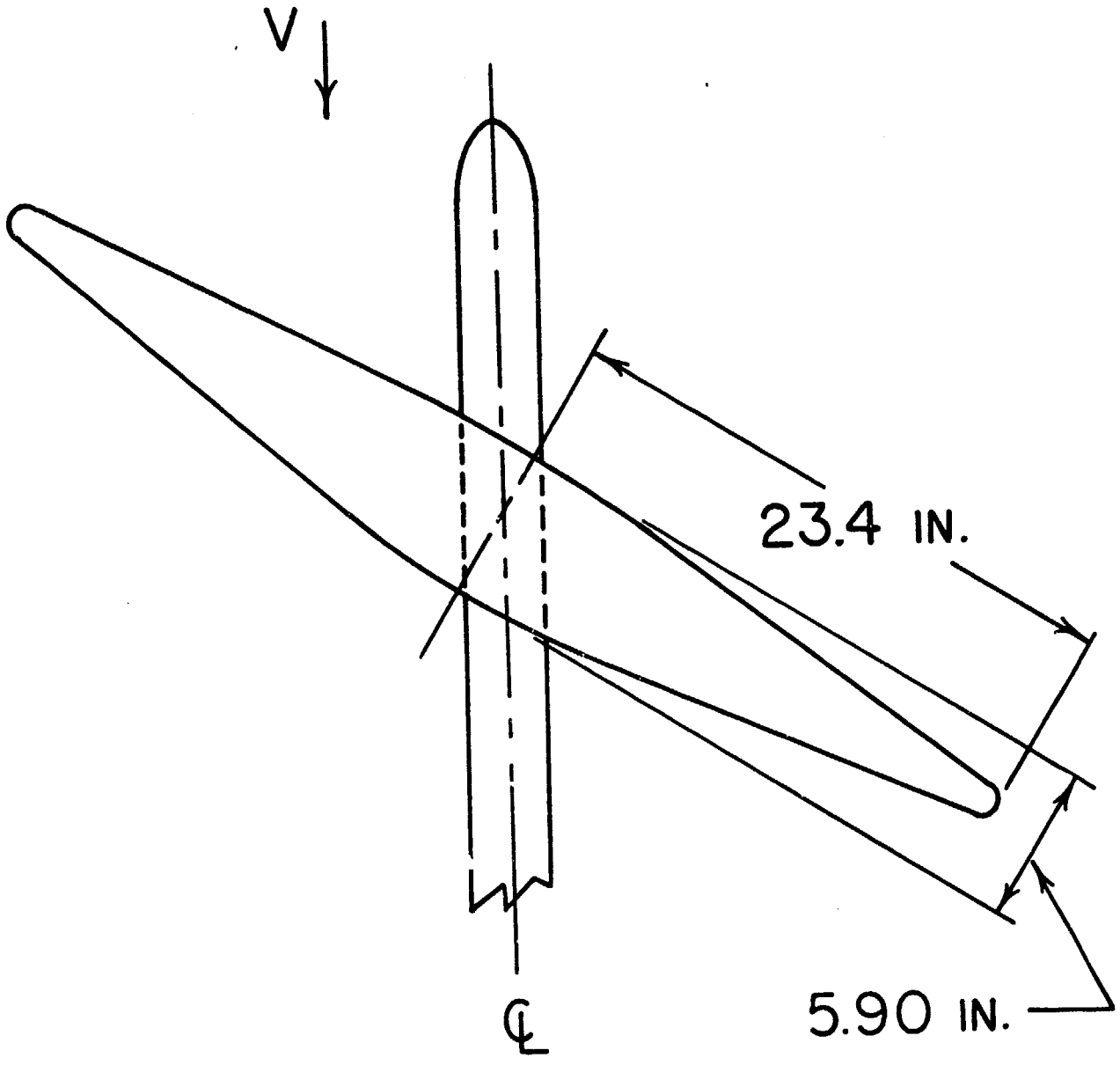
V
23.4 IN.
5.90 IN.
℄

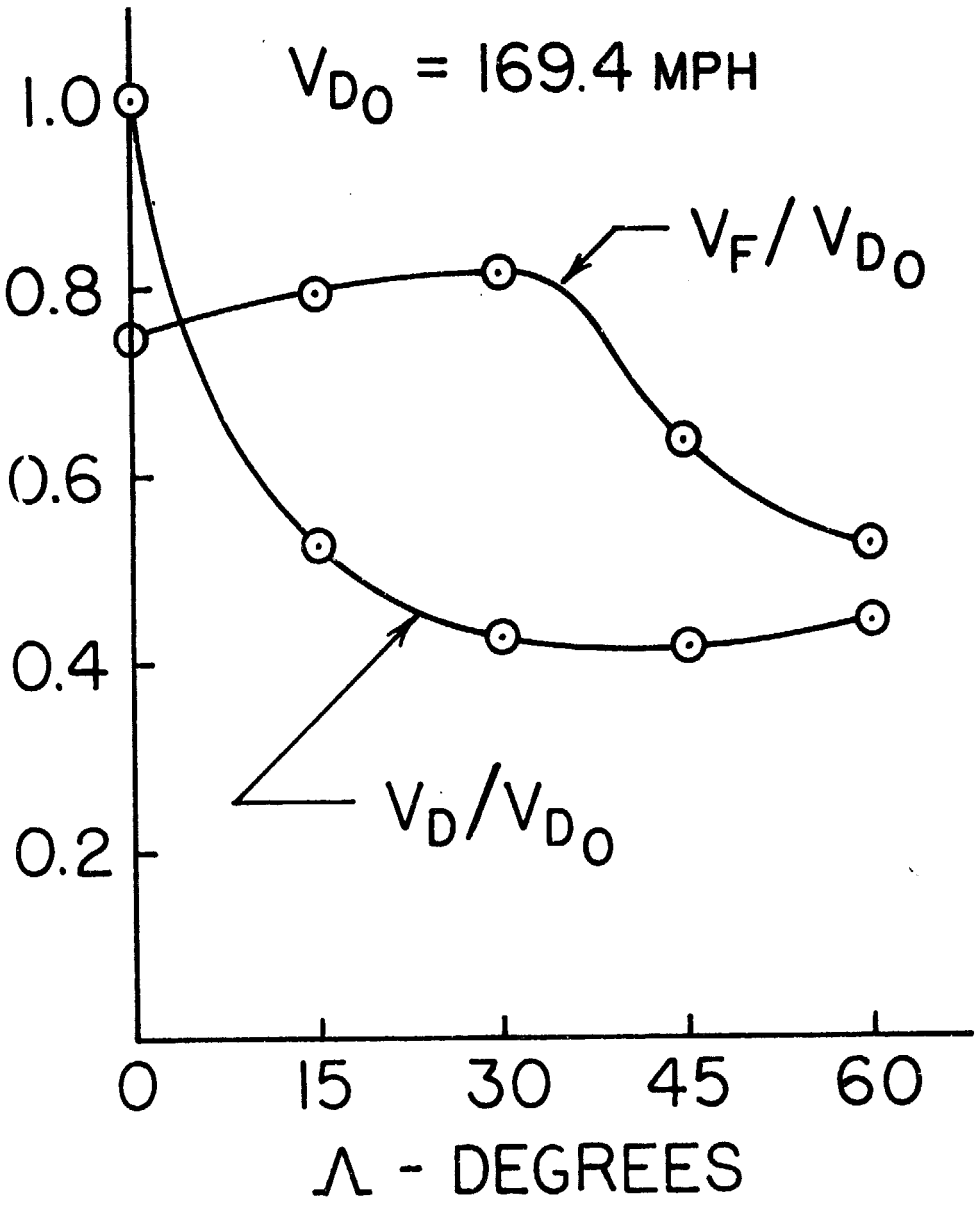
V_{D_0} = 169.4 MPH
1.0
0.8
0.6
0.4
0.2
V_F / V_{D_0}
V_D / V_{D_0}
0
15
30
45
60
Λ - DEGREES

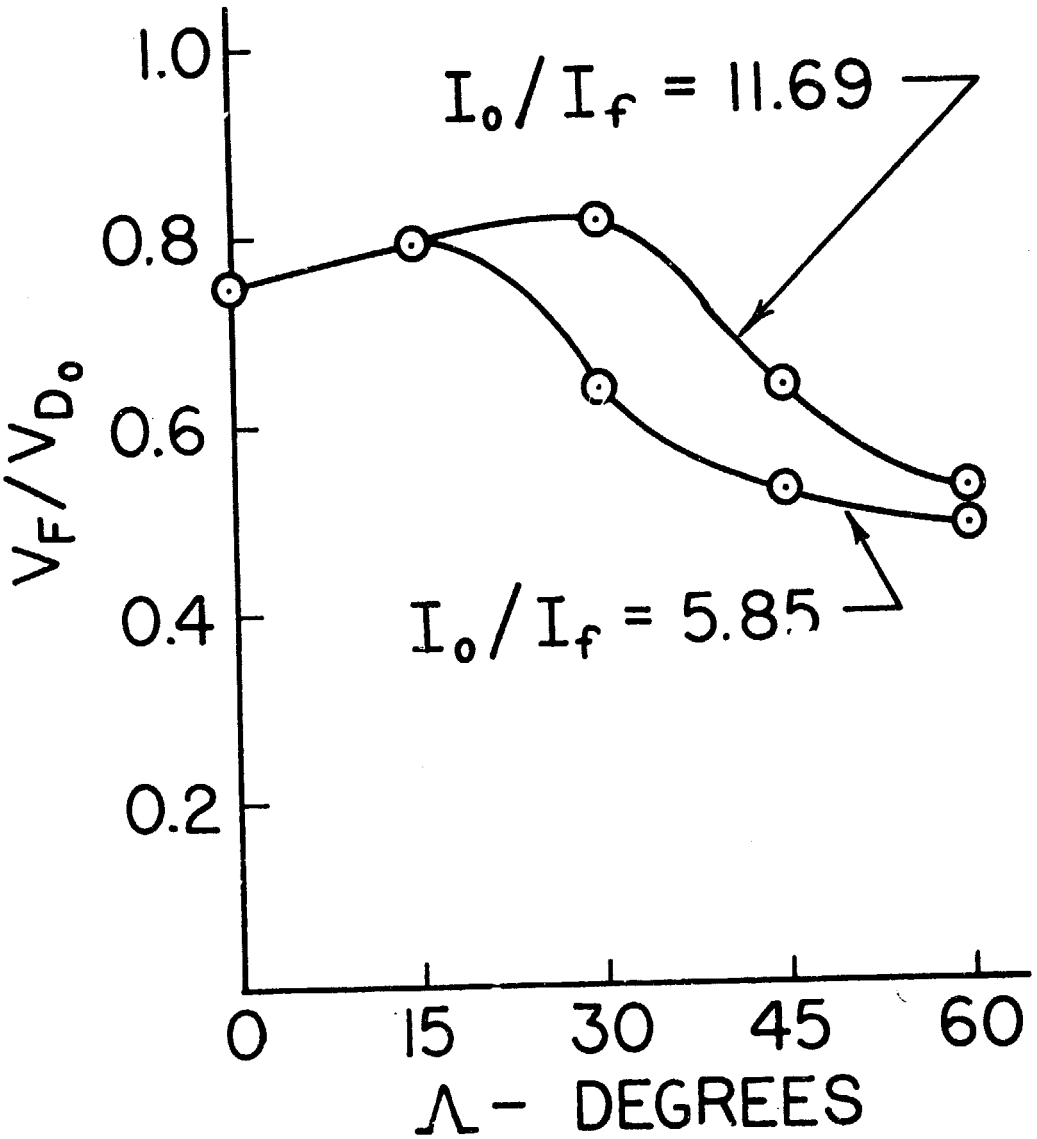
1.0
0.8
0.6
0.4
0.2
V_F / V_{D_0}
$I_0 / I_f = 11.69$
$I_0 / I_f = 5.85$
0
15
30
45
60
Λ - DEGREES

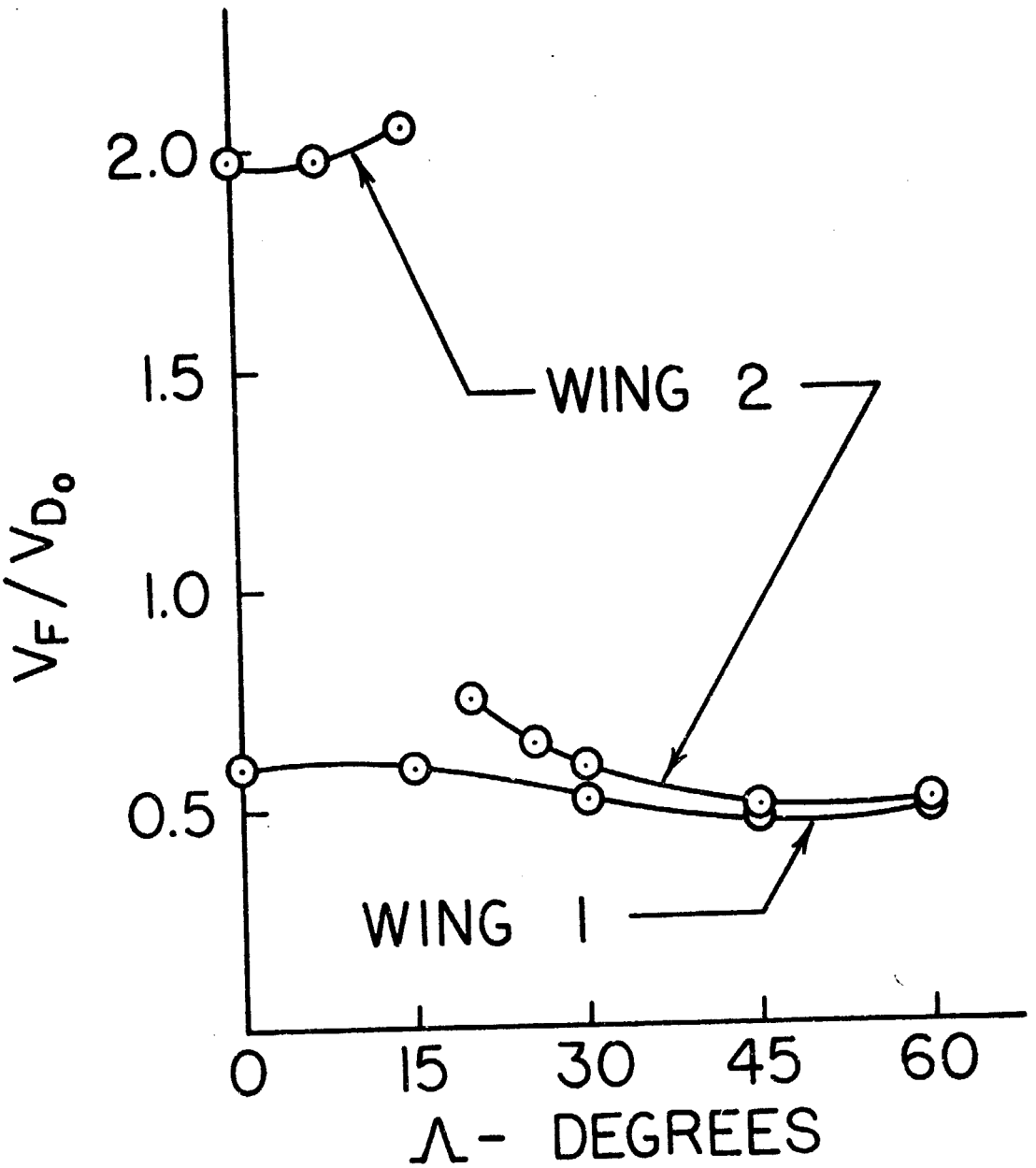
2.0
1.5
1.0
0.5
V_F / V_{D_o}
WING 2
WING 1
0
15
30
45
60
Λ - DEGREES

LATERAL EQUILIBRIUM OF ASYMMETRICALLY SWEPT WINGS - AILERON CONTROL VS. GEOMETRIC TWIST

Terrence A. Weisshaar*

Virginia Polytechnic Institute

and State University

Blacksburg, Virginia

This research was supported by NASA Ames Research Center, Moffett Field, California under NASA Grant NSG-2016.

Index categories: Aircraft Handling, Stability and Control; Aeroelasticity; Aircraft Structural Design.

*Assistant Professor, Aerospace and Ocean Engineering Department, Member AIAA.

Abstract

A static aeroelastic phenomenon unique to an aircraft with asymmetrically swept wings is discussed and the potential magnitude of its importance assessed. For this assessment, a simple formula is derived from the analysis of a highly idealized model. The validity of this formula is examined through the use of a more sophisticated numerical analysis. Among the results of this analysis are the following: aileron settings of a few degrees are sufficient to trim such aircraft in roll for 1g flight; the use of so-called built-in twist in the form of an initial wing anhedral provides an efficient alternative to aileron trim; if the wing is elastically tailored in a proper fashion, it may be possible to design a wing whose elastic deformation under airloads provides a form of self-trim in roll at the cruise q of the aircraft, in which case no aileron input or anhedral is necessary.

Introduction

The oblique wing aircraft concept is currently being explored as a possible method of achieving high lift-to-drag (L/D) ratios at high transonic and low supersonic speeds (Ref 1,2). Prominent among the features of this unconventional aircraft is a wing of relatively large unswept aspect ratio (of the order of 8-12) which can be pivoted so that it presents itself at an oblique angle to the flow (Fig. 1). Theoretically, this asymmetrical sweeping of a high aspect ratio wing results in a very efficient wing shape in this speed range (Ref. 3). That this theory is valid has been shown in wind tunnel tests at the NASA Ames Research Center (Ref. 4). While demonstrably advantageous to the aerodynamicist, such a design suggests potential structural stiffness and strength difficulties which deserve careful consideration. Of these difficulties, the areas of static aeroelasticity and flutter behavior of the wing seem most important and worthy of analysis.

The term static aeroelasticity is commonly applied to aeroelastic problems where inertia effects can be safely neglected. Control effectiveness and the redistribution of airloads on a flexible aircraft are prime examples of problems where the equilibrium state of the flight vehicle is highly dependent upon the interaction between the airloads and the flight structure. On the other hand, static wing divergence provides an example of a static aeroelastic stability problem. Since this latter problem is of no concern to a freely flying oblique winged aircraft (Ref. 2), the attention of this paper will be focused only on the problem of flexible wing airload redistribution and the lateral trim requirements of flexible wings which are asymmetrically swept.

Earlier studies have focused attention of stability and control characteristics which might be of importance to oblique wing aircraft design (Refs. 5, 6,7). In Ref. 7, the author very briefly explored the possible influence of

static aeroelasticity on oblique wing design. Further work in this area has shown that the analysis presented in that reference can be extended and interpreted in such a way as to yield meaningful results. For this reason, the present study is divided into three parts: the analysis of the potential aileron control requirements for an oblique winged aircraft to ensure lateral equilibrium at various flight speeds; the presentation, analysis and comparison of an alternative mode of ensuring lateral equilibrium, the use of so-called built-in or geometric twist; and, finally, an assessment of the validity of the assumptions used and results obtained in the latter two studies.

Discussion

Some insight into the magnitude and importance of the oblique wing lateral trim problem can be obtained through the study of the simplistic elastic wing model considered in Ref. 7. The analysis of this model, shown in Fig. 2, will seek to determine the extent to which aileron deflection, or some other means of control, is necessary to ensure lateral equilibrium. Although the analysis of the use of aileron deflection for this same model has been briefly discussed in Ref. 7, the essential features of that analysis will be reviewed here and the results extended because they bear heavily upon the ensuing geometric twist analysis.

The idealization shown in Fig. 2 represents a continuous, uniform-property, elastic wing, of constant chord, swept at an angle Λ to the direction of flight. The wing is uncambered and has full-span ailerons for lateral control. For the formulation of the analytical model, the wing is assumed to behave as a slender beam with a straight elastic axis; torsional flexibility of the wing is ignored to simplify the analysis. Finally, aerodynamic strip theory is used to describe both the applied loads and the aeroelastic loads. With reference to Fig. 2, the governing differential equation of equilibrium of the flexible wing, under the usual elementary beam theory assumptions can be written (in

nondimensional form (cf. Ref. 8, pp. 479-481) as:

$$\frac{d^4w}{d\eta^4} + \lambda \frac{dw}{d\eta} = \frac{p_o L^3}{EI} + \beta\delta(\eta) \qquad -1 \leq \eta \leq 1 \tag{1}$$

where $w(\eta)$ = bending deformation, nondimensionalized with respect to L.

p_o = constant load per unit length in the η direction.

EI = bending stiffness, a constant.

λ = $qcc_{L\alpha}L^3 \sin\Lambda \cos\Lambda/EI$.

β = $qcc_{L\delta}L^3 \cos^2\Lambda/EI$.

q = dynamic pressure.

$c_{L\alpha}$ = two-dimensional sectional lift curve slope per unit chordwise angle of attack.

$c_{L\delta}$ = two-dimensional sectional lift curve slope per unit aileron deflection.

If this wing were to be clamped at its center, a roll moment would be generated if ailerons were not applied in an antisymmetrical manner. This roll moment occurs because of the well-known tendency of sweptforward wings to develop lift forces when deflected upward and the tendency of sweptback wings to lose lift when similarly deflected upward. In the wind tunnel, a wing roll moment can be counteracted by the tunnel mount; in free flight, some mode of lateral control must be used. The analysis which follows assumes that longitudinal trim is supplied by control surfaces which do not enter this problem.

As shown in Ref. 7, the full span ailerons may be used to null out the aeroelastic roll moment on the oblique wing if they are deflected such that the following relation is satisfied.

$$\delta(\eta) = \begin{cases} \delta_o & 0 \leq \eta < 1 \\ -\delta_o & -1 \leq \eta < 0 \end{cases} \tag{2}$$

Moment equilibrium about the roll axis requires that

$$\delta_o = \left(\frac{c_{L\alpha}}{c_{L\delta}}\right)\tan\Lambda \int_{-1}^{1} \frac{dw}{d\eta} \tag{3}$$

The assumption of the existence of a very stiff wing pivot support structure at the aircraft centerline allows one to separate Eq. 1 into two regions, thus simplifying its solution. In this case, each wing half is assumed to be clamped at the aircraft centerline, or wing root position, and free of bending moments and shear at the wingtips. With these assumptions, a closed-form solution for δ_o in Eq. 3 may be found. Because the term $dw/d\eta$ enters into the aeroelastic load computation, this derivative is of more significance than the deflection $w(\eta)$ itself. For this reason, the solution to Eq. 1 is usually presented in terms of the variable $\Gamma(\eta)$ where

$$\Gamma(\eta) = \frac{dw}{d\eta} \tag{4}$$

With the definition of $\Gamma(\eta)$ in Eq. 4, the solution for $\Gamma(r)$ is written symbolically as:

$$\Gamma(\eta) = \begin{cases} \Gamma_R(\eta) & 0 < \eta \leq 1 \\ \Gamma_L(\eta) & -1 \leq \eta < 0 \end{cases} \tag{5}$$

The functions $\Gamma_R(\eta)$ and $\Gamma_L(\eta)$ are given in the Appendix to this paper. Substitution of these expressions into Eq. 3 and subsequent integration yields an expression for δ_o.

$$\delta_o = \frac{p_o L^3}{\beta E I}\left(\frac{T_L - T_R}{T_L + T_R}\right) \tag{6}$$

The variables T_L and T_R are functions of the aeroelastic parameter λ and are also to be found in the Appendix.

It is found that, if the sweptforward wing portion is clamped at the root and in the absence of aileron application, the wing will undergo static divergence at a value of $\lambda = 6.33$ (Ref. 8, 311-317). The value of the parameter λ thus provides one measure of the influence of static aeroelasticity in this type of problem. A related parameter which is sometimes useful is the variable q^*. The parameter q^* denotes the ratio of the flight q to the divergence q, q_{DIV}:

$$q^* = q/q_{DIV} \tag{7}$$

If the variables Λ, EI, L and c are held fixed, then

$$q^* = \lambda/6.33 \tag{8}$$

The magnitude of the aileron deflection parameter δ_o may be conveniently examined if we look at the behavior of another parameter, γ, found from a manipulation of Eq. 6.

$$\gamma = 6.33 \left[\delta_o \Big/ (p_o L^3/EI) \right] \Big/ \left[c_{L\alpha} \tan \Lambda / c_{L\delta} \right] \tag{9}$$

A graph of γ versus q^* is given in Fig. 3. Two features of the relation shown in Fig. 3 are worthy of note. First of all, as q^* approaches the value 4.335, the parameter γ tends to an infinite value because, at this value of q^*, $T_L = T_R$. Also, it is seen that the value of γ is nearly equal to unity for values of q^* in the range $0 \leq q^* \leq 1.50$. If this latter observation is used, together with Eq. 9, then

$$\delta_o = \gamma \left(\frac{p_o L^3}{EI} \right) \left(\frac{c_{L\alpha}}{c_{L\delta}} \right) \tan \Lambda \Big/ 6.33 \qquad (10a)$$

or

$$\delta_o \cong \left(\frac{p_o L^3}{EI} \right) \left(\frac{c_{L\alpha}}{c_{L\delta}} \right) \tan \Lambda \Big/ 6.33 \qquad (10b)$$

Eq. 10b can be rendered more meaningful if p_o is related to the 1g flight condition of an aircraft of gross weight W. p_o represents the load per unit length (assumed constant) along the swept span caused by the airloads on the rigid wing; a relation between p_o and W is readily obtained if we ignore both the aileron induced airloads and the aeroelastically induced airloads. This relation is

$$2p_o L \cong W \qquad (11)$$

Therefore, the first coefficient in Eq. 10b becomes

$$\frac{p_o L^3}{EI} \cong \frac{WL^2}{2EI} \qquad (12)$$

The degree to which Eq. 12 is an approximation will be discussed later. However, it should be remarked here that the inclusion of aeroelastic lift into the analysis causes the term on the left hand side of Eq. 12 to be a fraction of the term on the right. This fraction is very close to unity for reasonable values of q*. By substitution of Eq. 12 into Eq. 10b, one obtains the result:

$$\delta_o \cong \left[\frac{WL^2}{EI} \right] \left[\frac{c_{L\alpha} \tan \Lambda}{c_{L\delta}} \right] \Big/ 12.66 \text{ (radians)} \qquad (13)$$

The most striking feature of Eq. 13 is that δ_o does not depend on the dynamic pressure and therefore is not an explicit function of the flight speed. The

parameter δ_0 does, however, depend upon the wing flexibility and the sweep angle Λ. Although formulated for a 1g flight condition, the weight W enters the equation linearly and could just as well have been written as NW for an Ng condition. This feature of Eq. 13 means that, once the aircraft is trimmed for one flight speed at a given sweep angle Λ, it is trimmed for all flight speeds at that same sweep angle and altitude. To illustrate the order of magnitude of the aileron deflection which might occur for a large transport aircraft, let us use the following data which are chosen to be typical of this class of aircraft.

$W = 400{,}000$ lb.

$EI = 20.0 \times 10^{11}$ lb-in.

$\frac{C_{L\alpha}}{C_{L\delta}} = 2.5$

$L = 1200$ in.

For this data, we obtain, from Eq. 13:

$$\delta_0 \cong 3.26 \left[\tan \Lambda \right] \text{ (degrees)} \qquad (14)$$

At 45° of sweep, a full-span asymmetrical aileron deflection of 3.26° is necessary to ensure lateral equilibrium. Although not extremely large, such a deflection might have an adverse effect on aircraft yaw trim and cruise L/D.

Turning to the second objective of this paper, the previous discussion has illustrated but one method of controlling the tendency of the oblique wing to develop a rolling moment in flight. One method of improving aerodynamic performance in aircraft has been the use of geometric angle of attack distributions or "built-in twist." For this application, the flight structure is geometrically tailored to satisfy some performance objective.

Wind tunnel tests of "rigid" oblique wings and the analysis of such wings by methods employing accurate aerodynamic theories have shown that there is a tendency for the lift distribution to build up on the sweptback wing. This

tendency causes a roll moment opposite in direction to that caused by aeroelastic effects. To cancel out this adverse situation, it has been proposed that some amount of upward wing geometric curvature or dihedral be used to alleviate this roll moment (Ref. 9).

To understand how a swept wing with a built-in deflection can develop an angle of attack with respect to the airstream, consider the situation shown in Fig. 4 (the reader is referred to a similar, more complete discussion given in Ref. 10, pp. 474-479). Since small rotations transform as vector quantities, it is seen that the angle of attack α, seen by the freestream parallel to the flight direction is, for a sweptback wing section, given by the expression

$$\alpha = \theta \cos \Lambda - \psi \sin \Lambda \tag{15}$$

For a sweptforward wing, the above relation is modified by substitution of a "plus" sign for the negative sign before the second term on the right hand side.

If θ, the twist angle along the swept axis, is zero then the inclination of a sweptback wing such that the swept axis forms an angle ψ with the horizontal plane, i.e. a dihedral, results in a constant negative angle of attack along the wing. Conversely, a dihedral on a sweptforward wing results in a constant positive angle of attack. Thus, for an oblique wing, a built-in dihedral angle tends to generate a set of lift forces which roll the aircraft so as to elevate the sweptforward wing tip; an anhedral would produce just the opposite effect. The key point here is that the anhedral-dihedral effect is, in essence, a built-in geometric twist effect. The purpose of the ensuing discussion is to show how this effect can provide lateral equilibrium without any aileron action.

With the assumptions used in the previous aileron study and once again using chordwise cross sections, the nondimensional governing equation of equilibrium for the flexible wing with an initial built-in dihedral angle

distribution $\psi(\eta)$ ($\psi(\eta)$ is the angle formed by the swept axis and the horizontal plane) is as follows:

$$\frac{d^4w}{d\eta^4} + \lambda \frac{dw}{d\eta} = \frac{p_o L^3}{EI} - \lambda\psi(\eta) \qquad -1 \leq \eta \leq 1 \tag{16}$$

The definitions of the quantities other than $\psi(\eta)$ used in Eq. 16 are identical to those used in Eq. 1. To cancel the aeroelastic roll moment, a constant initial built-in anhedral angle is used such that $\psi(\eta)$ is defined as:

$$\psi(\eta) = \begin{cases} +\psi_o & -1 \leq \eta < 0 \\ -\psi_o & 0 < \eta \leq 1 \end{cases} \tag{17}$$

The comparison of Eqs. 16 and 17 with Eqs. 1 and 2 shows that they are made identical if

$$\psi_o = \delta_o \left(\frac{c_{L\delta}}{c_{L\alpha}} \right) \Big/ \tan \Lambda \tag{18}$$

To guarantee roll moment equilibrium, ψ_o must satisfy the relation

$$\psi_o = \int_{-1}^{1} \eta \frac{dw}{d\eta} d\eta = \int_{-1}^{1} \eta \, \Gamma(\eta) \, d\eta \tag{19}$$

The solution for the variable $\Gamma(\eta) = \frac{dw}{d\eta}$ in this problem is identical to that presented for the previous aileron problem if the term $\lambda\psi_o$ replaces the term $\beta\delta_o$ in the expressions for Γ_R and Γ_L given in the Appendix. Substitution of these expressions into Eq. 19 and subsequent integration yields a relation for ψ_o given by:

$$\psi_o = \frac{1}{\lambda} \left[\frac{p_o L^3}{EI} \right] \left[\frac{T_L - T_R}{T_L + T_R} \right] \tag{20}$$

The expressions for T_L and T_R are those presented in the Appendix.

Assumptions similar to those given for the aileron analysis lead us to an approximation for Eq. 20 given by:

$$\psi_o = \frac{1}{12.66}\left[\frac{WL^2}{EI}\right] \tag{21}$$

An examination of Eq. 21 and comparison of this relation with Eq. 13 reveals how remarkably efficient the use of built-in twist, in the form of the initial anhedral, is for the oblique wing roll equilibrium problem. Eq. 21 has no factor $(c_{L\alpha}/c_{L\delta})\tan\Lambda$, reflecting the fact that the same airfoil sections which are causing the roll equilibrium problem are also being used for its solution. As the influence of aeroelasticity increases with the angle of sweep, so too does the counteracting built-in twist effect, since the sine of Λ in Eq. 15 increases with Λ.

From Eq. 21, it is seen that the anhedral angle of the swept axis is not a function of flight speed. Use of the same typical parameters as were considered for the aileron example results in a value for ψ_o of

$$\psi_o = 1.30 \text{ degrees} \tag{22}$$

This initial anhedral angle is small and corresponds to a situation where the wing tips are initially located a distance of 27.2 inches below a horizontal plane passing through the fuselage centerline, a rather small distance when compared to the 100 foot semi-span.

Since the simplistic formulas given by Eqs. 13 and 21 are approximations, even for the idealized model used in this analysis, two additional tasks remain before this study can be considered complete. The first of these tasks is the determination of the extent to which the aeroelastic lift contribution affects the accuracy of these strip theory expressions. The second task is to

determine to what extent the use of aerodynamic strip theory to describe the loads affects the problem solution. For the sake of brevity, we will examine only the geometric twist problem, since the solutions to this problem and to the aileron problem are mathematically similar.

To accomplish the first task, we begin by summing all of the vertical forces which act upon the idealized wing and the equate these forces to the aircraft gross weight; the following expression results.

$$2\frac{p_o L^3}{EI} - \lambda \int_{-1}^{1} \frac{dw}{d\eta}\, d\eta = \frac{WL^2}{EI} \tag{23}$$

The integral term in Eq. 23 represents the relative vertical distance between the wing tips. Physical reasoning leads one to expect that this will be a small negative quantity. It is this latter term which is ignored in the formulation of Eqs. 12 and 20.

Direct integration of the integral term in Eq. 23 using the expressions for $\Gamma(\eta)$ and subsequent solution for p_o yields the relation:

$$\frac{p_o L^3}{EI} = \frac{WL^2}{2EI}\left[\frac{T_L + T_R}{T_R U_L - T_L U_R}\right] \tag{24}$$

U_L and U_R are defined in the Appendix. The substitution of Eq. 24 into Eq. 20 gives the exact solution for ψ_o:

$$\psi_o = \frac{1}{2\lambda}\left[\frac{T_L - T_R}{T_R U_L - T_L U_R}\right]\left[\frac{WL^2}{EI}\right] \tag{25}$$

The coefficient of the factor $\left[WL^2/EI\right]$ is a function of the aeroelastic parameter λ. Eq. 21 approximates the value of this coefficient to be 1/12.66 or 0.07900. This approximation is the result of taking the value of γ to be unity and ignoring the aeroelastic lift. The ratio $\psi_o/(WL^2/EI)$ is shown in

precluded. Even more important is the realization that the use of strip theory results in the overestimation of loads towards the wing tips.

To investigate these possible shortcomings an analysis, based upon the theoretical model developed in Ref. 11, was carried out. The aerodynamic theory used in Ref. 11 is based upon a modification of the Weissinger-L method detailed in Ref. 12. The structural model assumes the wing to be a beam with bending-torsion flexibility. The analysis method detailed in Ref. 12 is a matrix method which permits spanwise variations in wing elastic properties; its chief advantages are the ease with which it may be programmed for the computer and the relatively short computer run times needed for static aeroelastic analysis.

To test the validity of the simplistic relations derived previously in this paper, a computer study using the model just described was conducted on an elastic wing model similar in size to a set of elastic wings used in wind tunnel tests at Virginia Polytechnic Institute (Ref. 13). The idealized model has the following properties:

c = 4 inches

L = 20 inches

c_{L_α} = 6.28 per radian

EI = 1000.0 lb-in.

The torsional stiffness input to the computer program was chosen to be ten times the bending stiffness so that only bending flexibility was important to the analysis. The results of the analysis of this idealized, uncambered wing give the value of the initial built-in anhedral in terms of the wing loading parameter, W/S lb/ft^2. Given the scale of the idealized wing model, a value of W/S of the order of 1 to 2 psf. is probably representative when compared with the large transport data given previously. For this small model, the use of Eq. 21 gives an anhedral value of

$$\psi_o = 2.012 \times \left(\frac{W}{S}\right) \quad \text{degrees} \tag{27}$$

The above mentioned computer analysis was run at a Mach number of zero and at three sweep angles, $\Lambda = 15°$, $30°$ and $45°$. The studies were run for q* values in the range $0 \leq q \leq 2.5$. Attention is called to the fact that q_{DIV} changes with Λ. The results of this study are displayed in Fig. 6.

In Fig. 6, the required anhedral angle (per unit W/S psf.) is plotted versus q* for the three sweep angles considered. A solid straight line is drawn to represent the strip theory prediction. From this figure, it is seen that at each value of Λ, the required value of ψ_o is a function of q*. The change in required ψ_o is dramatic in the range $0 \leq q^* \leq 0.50$, but less so above $q^* = 0.50$. In all cases the strip theory formula overestimates the required value of ψ_o; the reason for this overestimation is that the use of strip theory results in an idealization that is too flexible from a static aeroelastic standpoint. That this latter observation is true can be seen in the fact that strip theory underestimates the value of q_{DIV} by about 30% when compared to the numerical method being used here.

Of further interest is the observation that, at low values of q*, a negative value of ψ_o is required. This corresponds to the observation in Ref. 9 that some slight upward curvature of the wing is necessary to correct a small roll moment caused by the lift distribution shifting toward the downstream wing tip. These small values of q* correspond to what the author would term a "rigid" wing.

Some potential importance may be attached to the fact that crossover points exist in the curves presented in Fig. 6 where the required anhedral changes sign. It is to be noted that these changes in sign occur at progressively larger values of q* as Λ increases. At this point, by definition, no lateral trim is required to maintain equilibrium. This occurs because the roll

moment caused by the airload buildup towards the sweptback wing tip is just cancelled by the aeroelastically induced load buildup towards the sweptforward wing tip. On an actual aircraft, this crossover or zero point would be a function of such parameters as wing planform shape, sweep angle, Mach number and stiffness distribution.

At the crossover point, no built-in anhedral or aileron action is necessary, no matter what the wing loading or load factor. The desirability of designing the wing so that the zero point occurs as closely to the cruise speed as possible, if not precisely at this speed,is obvious. Since so many other design objectives must be met by the structural engineer, this latter objective may be difficult to fulfill in practice.

Conclusions

Some unique static aeroelastic problems posed by the asymmetrical sweeping of a high aspect ratio wing have been examined through the use of a simplified model. Although the use of such an idealization to represent problems which are likely to occur in actual aircraft designs and the solutions to these problems is an oversimplification, the author nevertheless believes that several useful conclusions or guidelines may be drawn from this study.

The use of strip theory to represent aerodynamic and aeroelastic loads leads to answers which overestimate the amount of aileron input or geometric twist necessary to ensure lateral equilibrium, particularly at low values of q^*. In addition, the error introduced by strip theory increases as Λ increases. The simplistic formulas derived from strip theory assumptions thus give conservative results much as they do when used in conventional static aeroelastic stability studies.

The results derived through the use of more accurate aerodynamic theory show that as the parameter q* increases, increased demand is made on the method which guarantees lateral equilibrium. For small values of q* near zero, few demands are made to guarantee lateral equilibrium. The parameter q* can be made small, given a constant operating q, by increasing the clamped divergence q of the aircraft by one of several conventional methods; these methods include stiffening the structure or redistributing the wing area so that more of the area is inboard. For aircraft which are designed in a conventional manner to the usual strength and stiffness criteria, the amount of modification to preclude the roll problem discussed in this paper is probably minimal. The normal "droop" of an aircraft wing due to gravity provides some anhedral effect.

Of potential theoretical interest in the areas discussed in this paper is the use of structural modifications to further improve static aeroelastic performance. Modifications such as asymmetrical wing stiffening or redistribution of wing stiffness to bring the crossover or zero point near to the cruise q might prove to be worthwhile. A similar study of the use of various wing planforms and their relative merits might also be in order.

To summarize, this problem of asymmetrical wing static aeroelastic equilibrium is one which must certainly be considered by the designers of such an aircraft. It is likely, however, that after all the conventional design criteria are met, this additional unique criteria will cause few, if any, additional problems for this aircraft configuration.

References

1. Jones, R. T., "New Design Goals and a New Shape for the SST," Astronautics and Aeronautics, Vol. 10, No. 12, Dec. 1972, pp. 66-70.

2. Jones, R. T. and Nisbet, J. W., "Transonic Transport Wings - Oblique or Swept?," Astronautics and Aeronautics, Vol. 12, No. 1, Jan. 1974, pp. 40-47.

3. Jones, R. T., "Reduction of Wave Drag by Anti-symmetric Arrangements of Wings and Bodies," AIAA Journal, Vol. 10, No. 2, Feb. 1972, pp. 171-176.

4. Graham, L. A., Jones, R. T. and Boltz, F. W., "An Experimental Investigation of Three Oblique - Wing and Body Combinations at Mach Numbers Between 0.60 and 1.40," NASA TMX62, 256, April 1973.

5. Weisshaar, T. A. and Ashley, H., "Static Aeroelasticity and the Flying Wing," AIAA Journal of Aircraft, Vol. 10, No. 10, Oct. 1973, pp. 586-594.

6. Weisshaar, T. A. and Ashley, H., "Static Aeroelasticity and the Flying Wing, Revisited," AIAA Journal of Aircraft, Vol. 11, No. 11, Nov. 1974, pp. 718-720.

7. Weisshaar, T. A., "Influence of Static Aeroelasticity on Oblique Winged Aircraft," AIAA Journal of Aircraft, Vol. 11, No. 4, April, 1974, pp. 247-249.

8. Bisplinghoff, R. and Ashley, H., Principles of Aeroelasticity, Wiley, New York, 1962.

9. Graham, L. A., Jones, R. T. and Boltz, F. W., "An Investigation of an Oblique-Wing and Body Combination at Mach Numbers Between 0.60 and 1.40," NASA TM X62, 207, Dec. 1972.

10. Bisplinghoff, R. L., Ashley, H., and Halfman, R. L., Aeroelasticity, Addison-Wesley, Reading, Mass., 1955.

11. Gray, W. L. and Schenk, K. M., "A Method of Calculating the Subsonic Steady-state Loading on an Airplane with a Wing of Arbitrary Plan Form and Stiffness," NACA TN 3030, 1953.

12. Weissinger, J., "The Lift Distribution of Swept - Back Wings," NACA TM 1120, 1947.

13. Papadales, B. S., "An Experimental Investigation of Oblique Wing Static Aeroelastic Phenomena," Master of Science Thesis, Virginia Polytechnic Institute and State University, Blacksburg, Va., 1975.

TABLE I

q*	$\psi_o/(WL^2/EI)$ (Exact value)	Per cent error in approximate value	$(p_oL^3/EI)/(WL^2/2EI)$ (Exact value)
0.00	0.0750	+ 5.33	1.00
0.25	0.0751	+ 5.19	0.998
0.50	0.0753	+ 4.91	0.991
0.75	0.0756	+ 4.50	0.980
1.00	0.0761	+ 3.81	0.964
1.50	0.0776	+ 1.81	0.916
2.00	0.0797	- 0.878	0.846
2.50	0.0827	- 4.47	0.749
3.00	0.0867	- 8.88	0.618
3.50	0.0921	-14.2	0.444
4.00	0.0994	-20.5	0.207

The approximate value of $\psi_o/(WL^2/EI)$ is 0.0790.

APPENDIX

The analytical expressions for $\Gamma_L(\eta)$, $\Gamma_R(\eta)$, $T_L(\lambda)$, $T_R(\lambda)$, $U_L(\lambda)$ and $U_R(\lambda)$ used in the body of this paper are presented below. In the region $-1 \leq \eta \leq 0$, $\Gamma(\eta)$ is given by:

$$\Gamma_L(\eta) = \frac{1}{a^3}\left[\frac{p_o L^3}{EI} - \beta\delta_o\right] \times \left[1 - \frac{e^{-a(1+\eta)} + 2e^{a(1+\eta)/2}\cos f(1+\eta)}{e^{-a} + 2e^{a/2}\cos f}\right] \tag{A1}$$

where $a = \lambda^{1/3}$ and $f = a(3^{1/2}/2)$.

In the region $0 \leq \eta \leq 1$, $\Gamma(\eta)$ is given by:

$$\Gamma_R(\eta) = \frac{1}{a^3}\left[\frac{p_o L^3}{EI} + \beta\delta_o\right] \times \left[1 - \frac{e^{a(1-\eta)} + 2e^{-a(1-\eta)/2}\cos f(1-\eta)}{e^{a} + 2e^{-a/2}\cos f}\right] \tag{A2}$$

The expressions for T_L and T_R are given by:

$$T_L = \frac{e^{-3a/2} - \cos f + 3^{1/2}\sin f}{a^2(e^{-3a/2} + 2\cos f)} \tag{A3}$$

$$T_R = \frac{e^{3a/2} - \cos f - 3^{1/2}\sin f}{a^2(e^{3a/2} + 2\cos f)} \tag{A4}$$

The expressions for U_L and U_R are:

$$U_L = \frac{\cos f + 3^{1/2}\sin f - e^{-3a/2}}{a(e^{-3a/2} + 2\cos f)} \tag{A5}$$

$$U_R = \frac{\cos f - 3^{1/2}\sin f - e^{3a/2}}{a(e^{3a/2} + 2\cos f)} \tag{A6}$$

LIST OF FIGURES

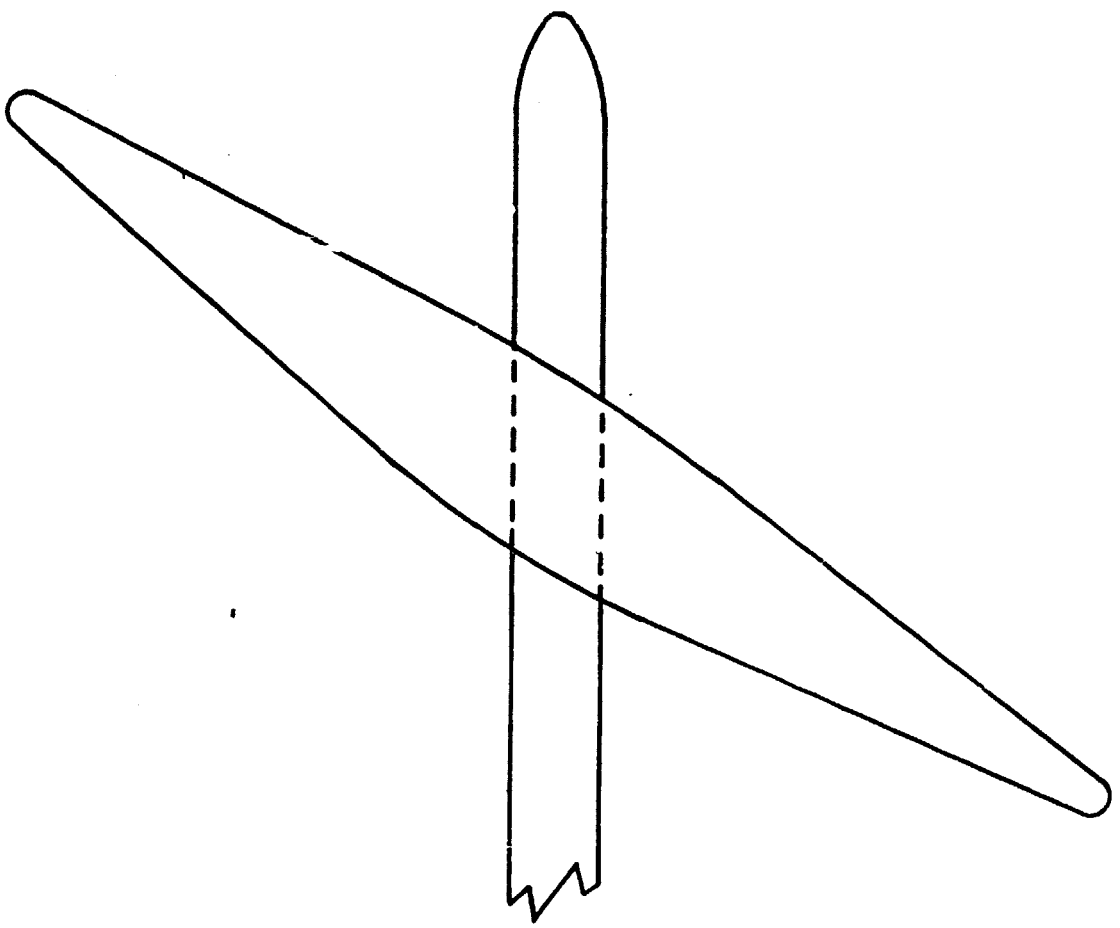

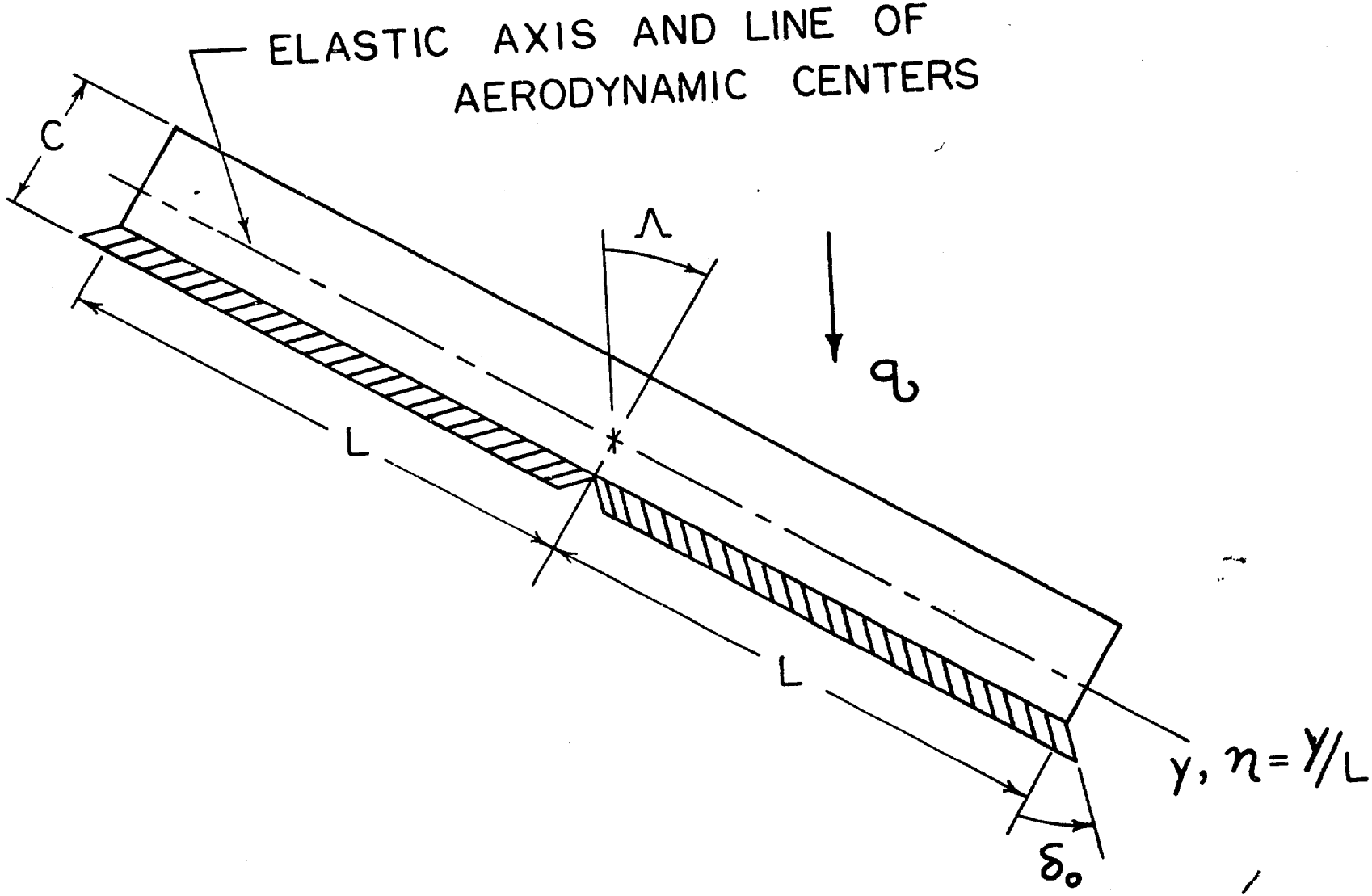
ELASTIC AXIS AND LINE OF
AERODYNAMIC CENTERS
C
Λ
q
L
L
y, η = y/L
δ₀

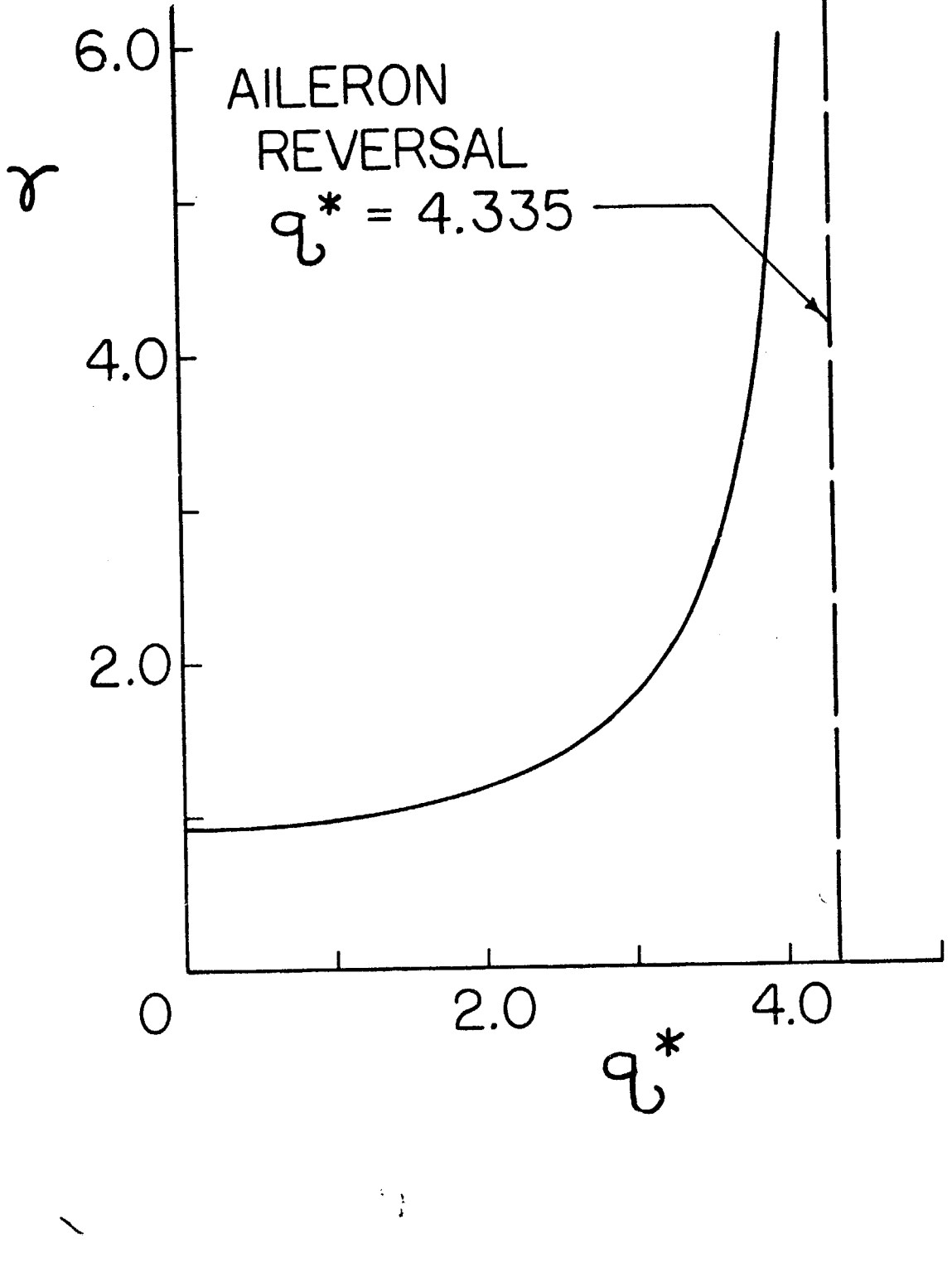
6.0
4.0
2.0
0
2.0
4.0
γ
q*
AILERON
REVERSAL
q* = 4.335

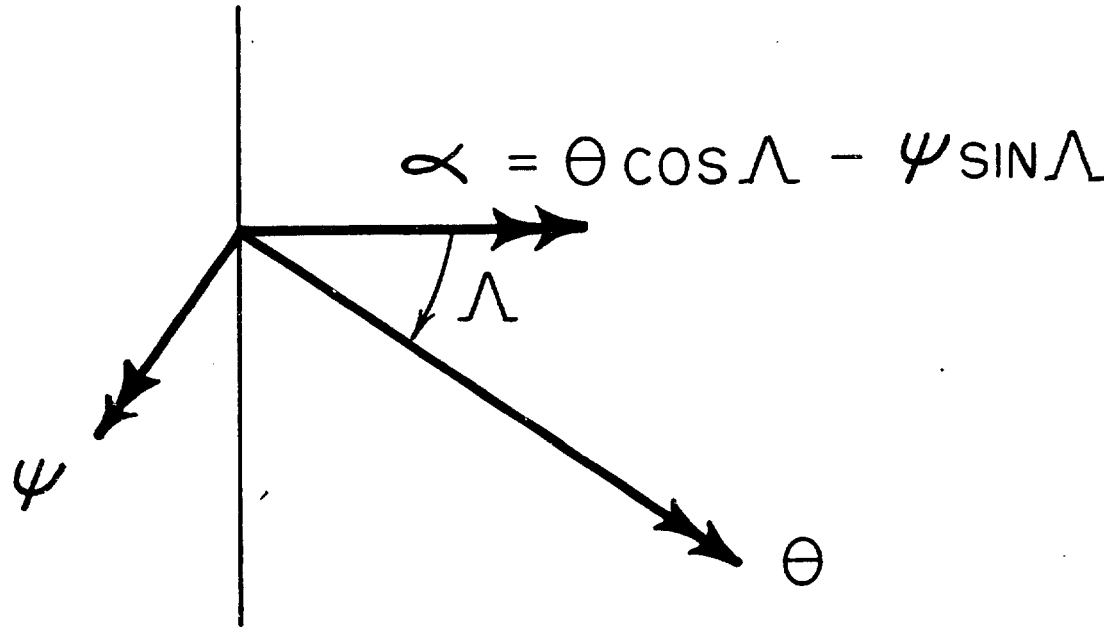
$\alpha = \theta \cos\Lambda - \psi \sin\Lambda$
Λ
ψ
θ

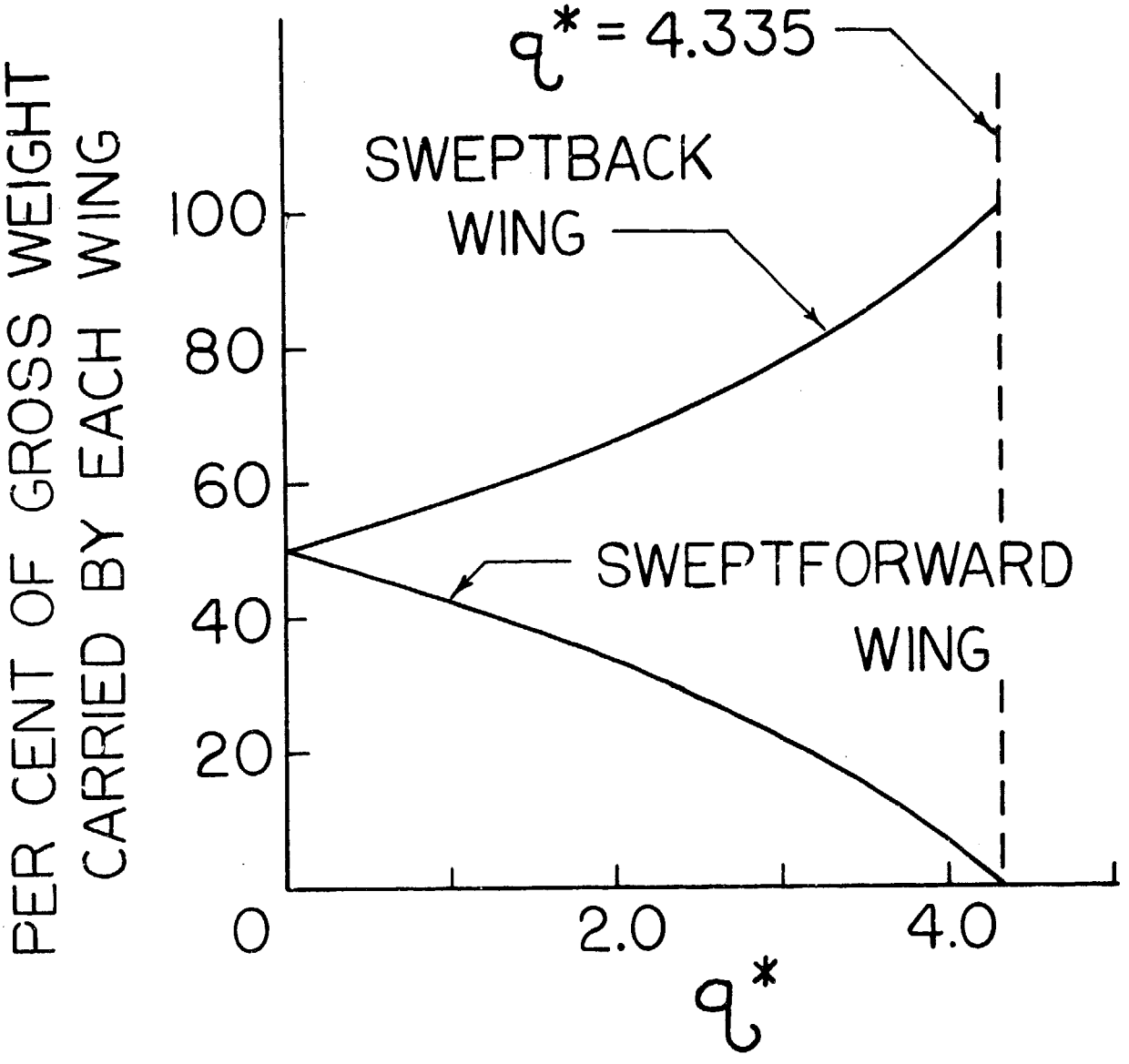
PER CENT OF GROSS WEIGHT CARRIED BY EACH WING
100
80
60
40
20
0
2.0
4.0
q*
q* = 4.335
SWEPTBACK WING
SWEPTFORWARD WING

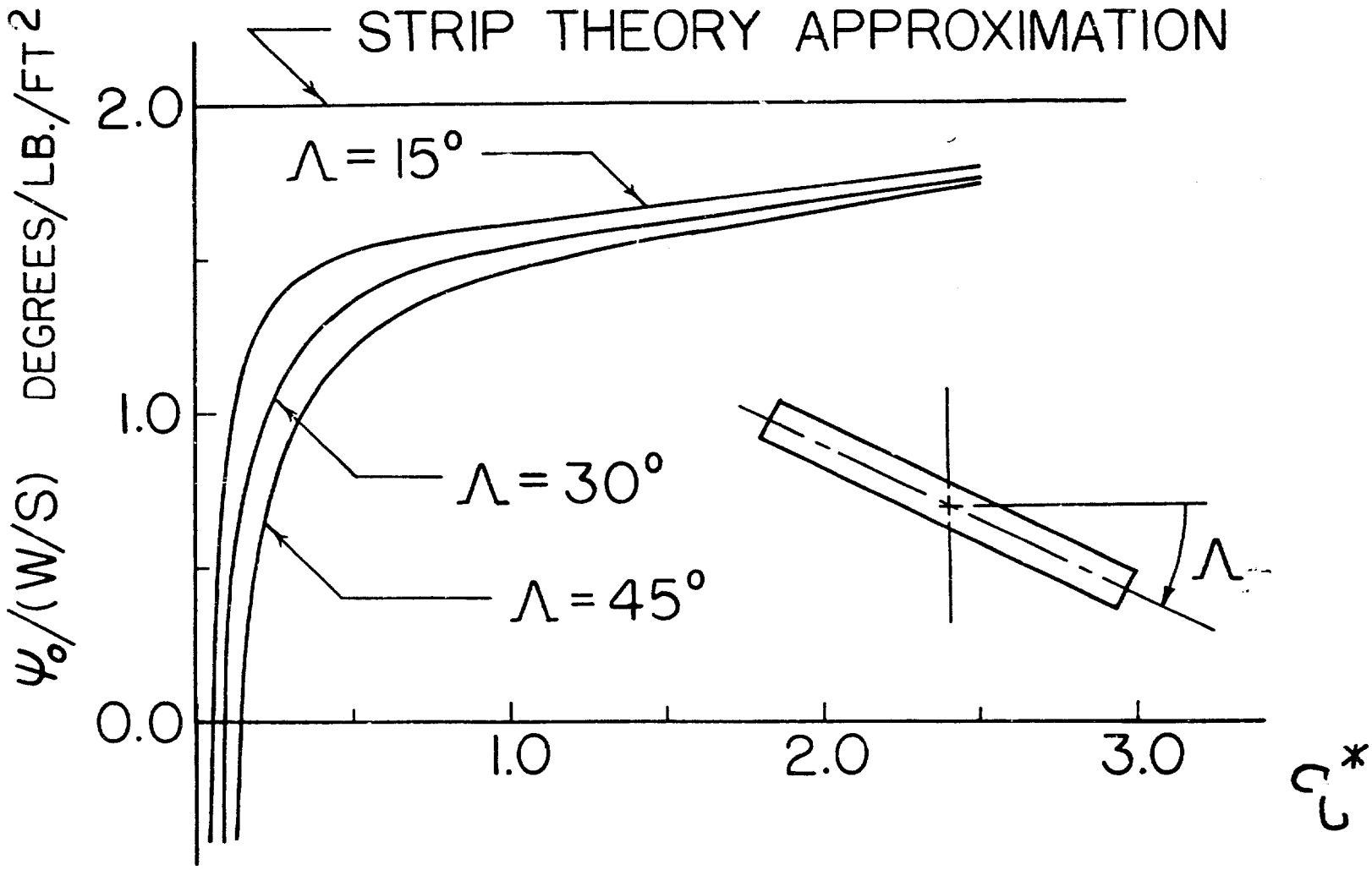
STRIP THEORY APPROXIMATION
$\psi_o/(W/S)$ DEGREES/LB./FT^2
2.0
1.0
0.0
$\Lambda = 15°$
$\Lambda = 30°$
$\Lambda = 45°$
Λ
1.0
2.0
3.0
C_L^*